Earth Syst. Dynam. Discuss., 4, 109–177, 2013
www.earth-syst-dynam-discuss.net/4/109/2013/
doi:10.5194/esdd-4-109-2013

Earth System Dynamics Discussions

Hydrological cycle over south and southeast Asian river basins as simulated by PCMDI/CMIP3 experiments

S. Hasson[1], V. Lucarini[1,2], and S. Pascale[1]

[1]Meteorological Institute, KlimaCampus, University of Hamburg, Hamburg, Germany
[2]Department of Mathematics and Statistics, University of Reading, Reading, UK

Received: 7 January 2013 – Accepted: 15 January 2013 – Published: 22 January 2013

Correspondence to: S. Hasson (shabeh.hasson@zmaw.de)

Published by Copernicus Publications on behalf of the European Geosciences Union.

Abstract

We investigate how CMIP3 climate models describe the hydrological cycle over four major South and Southeast Asian river basins (Indus, Ganges, Brahmaputra and Mekong) for the XX, XXI, and XXII centuries. For the XX century, models' simulated water balance and total runoff quantities are neither consistent with the observed mean river discharges nor among the models. Most of the models underestimate the water balance for the Ganges, Brahmaputra and Mekong basin and overestimate it for the Indus basin. The only modest inter-model agreement is found for the Indus basin in terms of precipitation, evaporation and the strength of the hydrological cycle and for the Brahmaputra basin in terms of evaporation. While some models show inconsistencies for the Indus and the Ganges basins, most of the models seem to conserve water at the river basin scale up to a good degree of approximation. Models agree on a negative change of the water balance for Indus and a positive change in the strength of the hydrological cycle, whereas for Brahmaputra, Mekong and Ganges, most of the models project a positive change in both quantities. Most of the models foresee an increase in the inter-annual variability of the water balance for the Ganges and Mekong basins which is consistent with the projected changes in the Monsoon precipitation. No considerable future change in the inter-annual variability of water balance is found for the Indus basin, characterized by a more complex meteorology, because its precipitation regime is determined not only by the summer monsoon but also by the winter mid-latitude disturbances.

1 Introduction

South and Southeast Asian economies are based on the agriculture and largely depend on the available freshwater resources. Presently, the region is facing increased water demands due to the burgeoning population and economic development. Sustainable freshwater supplies are therefore crucial for ensuring food security and economic wellbeing of 1.4 billion people living in the region. However, freshwater supplies obtained from the major South and Southeast Asian Rivers are highly variable in space and time, and this makes it hard to have an adequate water management and to support efficient agricultural practices. Providing suitable water storage capacity can act as an efficient adaptation to these issues, as it makes it possible to supply continuously water and enhance the capability to counter hydrological fast-onset disasters.

One of the most relevant aspects of observed and projected climate change is the variation of the hydrological cycle at global and regional scale, with the ensuing changes in the statistical properties and the seasonality of precipitation, evaporation, and runoff, and consequently in the discharge of the rivers. South and Southeast Asia is a hot spot of climate change and it is anticipated that changes in the hydrological cycle will be quite serious in this region. The potential adverse impacts of climate change can further exacerbate the existing water management problems and can influence the socio-economical balances of the region (IPCC, 2007). Therefore, in terms of public policy, water resource management and defense from hydrological risks cannot be decoupled from the climate change agenda. As example, in this region considering the future water availability under warmer climate conditions while planning new water reservoirs can be long-sighted, keeping in view the huge investment costs and that the lifetime of these reservoirs is comparable to the time scale over which significant changes in the hydro-climatology will be evident. It is then crucial for the policy makers and the regional actors to have high-quality information on the projected climate change in the area.

Atmosphere-ocean coupled general circulation models (GCMs) are the most powerful tools currently being used in the scientific community for studying climate variability and climate change. The hydrological cycle is one of the most relevant important aspects of climate, so that on the one side it is crucial for a GCM to represent it carefully for a myriad of applications, and on the other side tests of the representation of the hydrological cycle at regional and global scale constitute very relevant benchmark tests for GCMs. However, the accurate representation of the hydrological cycle and

ESDD
4, 109–177, 2013

its interaction with the other climatic processes is non-trivial in these climate models mainly because the hydrological components feature multi-scale properties, i.e. non-trivial dynamics occurs on a vast variety of spatial and temporal scales, including scales much smaller than those typically resolved explicitly by models. It has already been shown that it is far from trivial for GCMs to have a self-consistent and realistic representation of the hydrological cycle on regions scales – see, e.g. the case of the Danube (Lucarini et al., 2008) – and, recently, problems of self-consistency in the conservation of the total water mass have been observed also at global scale (Liepert and Previdi, 2012). It is important to underline that inconsistencies in terms of mass balance in the representation of the hydrological cycle imply inconsistencies in the energetics of the climate model (Liepert and Previdi, 2012; Lucarini and Ragone, 2011).

In view of the socio-economic importance of its freshwater resources, it is fundamentally urgent to investigate the ability of the present day climate models for the accurate representation of the hydrological cycle over South and Southeast Asia and to assess their response regarding future changes under the warmer climate. This investigation is helpful in getting reliable future estimates of the water balances in the region. Many studies have been performed in this regard (Kripalani et al., 1997; Kang et al., 2002; Annamalai et al., 2007; Lin et al., 2008) and associate the model biases with the inaccurate representation of the monsoon and its interaction with the westerly disturbances over the region. A recent study by Boos and Hurley (2012) links the misrepresentation of Hindu kush Karakoram Himalaya (HKH) topography by CMIP3 and CMIP5 models with biases in the dynamics and thermodynamics of the monsoonal circulation, with the resulting prevalence among models of negative precipitation anomalies and of delay in the Monsoon onset. Lin et al. (2008) discuss the spatial biases for the seasonal mean Asian summer monsoon precipitation in the CMIP3 models, showing that the reasonable performance of the models for the seasonal-mean Indian summer monsoon (60–100° E) precipitation features compensation between excessive near-to-equator precipitation and the insufficient precipitation far from the equator. Similarly, the biases are also associated with the onset and the magnitude of the monsoonal rainfall.

ESDD
4, 109–177, 2013

Clearly, biases in the models' representation of the spatial and temporal precipitation patterns hinder the possibility of performing very reliable impact assessment studies, and their applicability for informing effectively bodies responsible for the management of the water resources. Following Lucarini et al. (2008) we believe that the verification and validation of GCMs should additionally be performed at a river-basin scale, through accurately calculating the hydrological quantities within the basin boundaries, in order to characterize the models' behavior within the naturally defined geographical unit relevant for water management.

Large inter-model variability is one of the major weaknesses in ascertaining the future climate change projections. To synthesize the multi-model outputs, the so called ensemble mean approach is commonly used in various ways. The present study also discusses that interpreting the model results using this approach hides the model biases during the verification procedure and may be detrimental in interpreting the projections for the future changes in the hydrological cycle over the region.

In view of the discussed spatio-temporal biases in GCMs, this study first investigates the ability of Third Phase of the Climate Models Inter-comparison Phase of the Program for Climate Model Diagnosis and Inter-comparison (PCMDI/CMIP3, see http://www-pcmdi.llnl.gov/) (Meehl et al., 2004) in describing the hydrological cycle for four major river basins of South and Southeast Asia, namely those of Indus, Ganges, Brahmaputra and the Mekong. The annual mean and the deviations from the long-term mean are calculated for hydrological observables such as the basin integrated precipitation, evaporation, water balance, strength of the hydrological cycle, and runoff. We first consider the last 40 yr of the XX century and test the agreement of the GCMs outputs with historically observed quantities, focusing on the river discharge. Furthermore, the basin integrated simulated total runoffs (sub-surface and surface) are compared against basin integrated difference between precipitation and evaporation to verify whether the land modules of the climate models conserve water as discussed in Lucarini et al. (2008). In the second part, future changes in the same hydrological quantities for the last 40 yr of the XXI and of the XXII centuries with respect to the

ESDD
4, 109–177, 2013

XX century (1961–2000) are presented for the SRES A1B scenario. The SRES A1B scenario (720 ppm of CO_2 after 2100) is chosen as it represents the median of the rest of the IPCC scenarios in terms of the greenhouse gas forcing (GHG) (IPCC, 2007).

The results of this investigation provide a strong motivation in exploring possible future changes in the regional atmospheric circulations, i.e. monsoon and winter westerly mid-latitude disturbances, and consequently their impact on the hydrological cycle of the region. A follow up of this paper will deal with the intra-annual variability of the hydrological cycle in the same set of models. The paper is structured as follows: Sect. 2 describes the characteristics of the present day hydrology of the study region. Section 3 describes the data and the method adopted for the study along with its implications for the analysis. Section 4 discusses the results. Section 5 summarizes the findings, and Sect. 6 presents the conclusion.

2 Study region

The study region comprises of the four major river basins of South and Southeast Asia namely Indus, Ganges, Brahmaputra and the Mekong (see Fig. 1). These river basins have diverse hydrological regimes because of the diversity among the components defining their climate. These may include the variations in the latitude, longitude and altitude, regional climate patterns, the presence of sea, desert, HKH ranges and the highly concentrated cryosphere. The hydrology of these rivers depends on the moisture source from the Monsoon system and the westerly disturbances and dominates with the snow and glacier melt at the higher and the rainfall at the low altitudes. The eastern basins of the study area are comparatively wetter than the western basins. This is because the fact that the monsoon rainfall dominates in the summer months in the eastern part and gets weaker on the western side with a time delay of some weeks. In the west, westerly disturbances drop moisture in the winter months mainly in the form of solid precipitation (Rees and Collins, 2006). This effect is much weaker as we go east. Therefore, the melt water contribution is reported to be extremely important

Discussion Paper | Discussion Paper | Discussion Paper | Discussion Paper |

ESDD

4, 109–177, 2013

Hydrological cycle over south and southeast Asian river basins

S. Hasson et al.

for the Indus, important for the Brahmaputra, modest for the Ganges but the least important for the Mekong River (Immerzeel et al., 2010). Also the high variability and the positive west to east gradient in the snow coverage are observed across the Himalayas and the Tibetan Plateau (Immerzeel et al., 2009). Table 1 summarizes the general characteristics of the studied basins, whereas details of individual basins are discussed below.

Indus basin

The Indus River originates from the Tibetan Plateau (China) and drains through India, Afghanistan and Pakistan before its confluence to the Arabian Sea. The Indus basin is usually divided into an upper and a lower part at the point the river enters into the Tarbela reservoir in Pakistan. The hydrology is dominated by two major sources of moisture, i.e. monsoon and western disturbances. The annual precipitation ranges between 100–750 mm and is confined to the monsoon (July–September) and the winter seasons (December–March). The whole basin is classified into different zones, from humid and sub-humid in the north to the arid and the hyper-arid in the south. The observational record for the last 40 yr of the XX century suggests a statistically significant increase in the seasonal and annual precipitation within the Upper Indus Basin (UIB) (Archer and Fowler, 2004). However, there are conflicting signals how the regional warming will affect the hydrology of the basin and are characterized by the observed cooling in the recent decades (Fowler and Archer, 2005). However, ensembles of 13 and 17 CMIP3 GCMs suggest higher warming rates over the northwestern part of the basin than over the southern plains and against the respective global averages for SRES A2 and A1B scenarios respectively throughout the XXI century (Islam et al., 2009). Almost 80 % of the mean annual flows are confined to the summer months (April–September) with a peak in August. Such peak is due to the snow and glacier melt in the HKH region at high latitudes (roughly 35–38° N), and snow melt and monsoon rainfall at lower latitudes (roughly 30–35° N). The low flow period comes in the winter

ESDD
4, 109–177, 2013

months (October–March) and is attributed to the winter rainfall and the base flow. The agriculture sector consumes more than 95 % of the total water supply.

The average flows measured at Kotri, the last gauging site, are about 1250 $m^3 s^{-1}$. With 18495 glaciers covering an area of 21 000 km^2 (Bajracharya and Shrestha, 2011) and 13.5 % of an average snow coverage (Gurung et al., 2011), the Indus River has the highest melt water index as compared to other South and Southeast Asian rivers originating from the HKH region. Based on a modeling study, Immerzeel et al. (2010) reports that the normalized melt water index for the Indus is 151 % of the total discharge naturally generated downstream. The index is calculated as a ratio between the volume of the upstream snow and glacier melt runoff and the water balance of the basin naturally available downstream ($P - E$). The Indus basin has great importance for the food production and the wellbeing of about 260 million population estimated for the year 2010 (CIESIN, 2005).

Ganges basin

Originating from the Central Himalayan Range, the Ganges river drains across India, Nepal, Bangladesh and China before its confluence to the Indian Ocean at the Bay of Bengal. The river is highly regulated with dams and irrigation canals right after it enters into the plains near Haridwar (Bharati et al., 2011), usually for agriculture purposes. Agriculture has a share of almost 90 % of the river supplies to ensure the wellbeing of about 520 million people (CIESIN, 2005). The basin hydrology is dominated by the monsoon system. The mean annual precipitation corresponds to more than 1000 mm and has a high spatial variability. Almost 75 % of the annual rainfall occurs in the monsoon months (June–September). The observational record indicates that the precipitation in the basin is by-and-large stable (Mirza et al., 1998; Immerzeel, 2008). The mean flow for the period 1950–2008 is estimated as about 11000 $m^3 s^{-1}$ at the Hardinge Bridge, the last gauging site. These flows have a large inter-annual and intra-annual variability and feature the decreasing trend which may be attributed to the decrease in the strength of the Indian monsoon (Webster et al., 1998; Jian et al., 2009) and/or

ESDD
4, 109–177, 2013

some other factors. More than 85 % of the river flows are confined to the high flow period (July–October) with the mean maximum in late August due to heavy contribution from monsoon rainfall and the glacier melt. During the lean flow period (November–June) contribution comes from the snowmelt (April–June), winter rainfall and the base flow. The total number of glaciers 7963 cover an area of abut 9000 km^2 (Bajracharya and Shrestha, 2011) whereas the annual average snow coverage is about 5 % only (Gurung et al., 2011). A modeling study suggests the low melt water index i.e. only 10 % to the discharge available downstream (Immerzeel et al., 2010).

Brahmaputra basin

The Brahmaputra River originates from the southwestern part of the Tibetan Plateau and drains through China, India, Bangladesh and Bhutan. The river is the lifeline for approximately 66 million people (CIESIN, 2005). The hydrology is dominated by the influence of the monsoon system. The mean annual precipitation is similar to that of the Ganges basin, i.e. about 1000 mm, whereas upstream precipitation shows an increasing trend (Mirza et al., 1998) by 25 % (Immerzeel et al., 2009). The mean flow for the period 1956–2008 is calculated to be about 20 000 $m^3 s^{-1}$ at Bahadurabad. With characteristics of large seasonal and annual variability these river flows show an overall increasing trend. However, there is a clear decreasing trend since 1988. The analysis shows that more than 90 % of the flows are confined to the high flow period (April–early November) with a mean maximum in mid-July. The early rise of the hydrograph in April is attributed to the snow melt contribution which reduces in the late spring or in the early summer and is compensated by the glacier melt. The monsoon rainfall starts a couple of weeks earlier as compared to the Ganges basin (Webster et al., 1998; Jian et al., 2009) and spans from late May till September. The lean flow period comprises of the winter months only. In addition to 11 497 glaciers covering an estimated area of about 14 000 km^2 (Bajracharya and Shrestha, 2011), the basin has 20 % of the annual average snow coverage (Gurung et al., 2011). Brahmaputra has a melt water index of 27 % compared to the discharge generated downstream (Immerzeel et al., 2010).

ESDD
4, 109–177, 2013

Mekong basin

Draining through China, Myanmar, Lao PDR, Thailand, Cambodia and Viet Nam, the Mekong River is amongst the largest in the world. The hydrological regime of the Mekong Basin primarily depends upon the climatic conditions of the alternating wet and the dry seasons. The climate is governed by the northeasterly and the southwesterly monsoonal winds. The annual rainfall ranges between 1000–1600 mm in the dry region of northeast Thailand to 2000–3000 mm in the wet regions of the northern and eastern highlands. Almost 90 % of the annual rainfall is received under the southwest monsoon system between May and October (MRC, 2005; FAO, 2008). The dry season spans from November to April. The mean discharge is about 17 000 $m^3 s^{-1}$ at Pakse gauging site. Almost 90 % of the annual discharge takes place in the high flow season (June–November) with a peak in August, and the remaining 10 % in the low flow period (December–May). With only 482 glaciers covering an area of about 230 km^2 (Bajracharya and Shrestha, 2011) and about 3 % of average annual snow coverage (Gurung et al., 2011), melt water has a negligible contribution to the Mekong River. Eastham et al. (2008) suggests that in an extreme climate change scenarios where all the glaciers vanish by 2030, the Mekong would see an increase of only 80 $m^3 s^{-1}$ to the average discharge of 3500 $m^3 s^{-1}$ at the Chiang Saen site. The agricultural sector is the major consumer of freshwater (Johnston et al., 2010). Almost 79 million people (CIESIN, 2005) are directly dependent on the water supply from the Mekong River for their food, livelihood and the economic wellbeing.

3 Data and method

3.1 Method

Various tools and techniques are being used to study the potential hydrological changes under warmer climates at a basin scale based on the specific objectives of the study and the details of the information required. We have categorized these methods into three following groups and have discussed the usefulness of their applications:

1. Use of hydrological models coupled with a climate model output
2. Spatio-temporal analogue techniques
3. Direct or indirect use of global climate model(s') output.

The most commonly used approach to assess the hydrological sensitivity against the changes in the foreseen climate is to couple hydrological models with climate models. That itself may include various techniques like: (i) direct use of GCMs output as input to the hydrological models (Nijssen et al., 2001; Gosain et al., 2006; Immerzeel et al., 2010); (ii) high resolution climate information obtained through dynamical or statistical downscaling for an improved understanding of hydrological processes at a local scale (Christensen et al., 2004); (iii) considering hypothetical changes of increase/decrease in the relevant quantities as input to the hydrological models (Singh and Kumar, 1997; Singh and Bengtsson, 2004; Singh et al., 2006) etc.

The dynamical downscaling through using the Regional Climate Models (RCMs) is a common approach to attain a higher resolution representation of the hydrological cycle. Such methods are computationally expensive and largely depend on the skill of the driving GCM, and they may introduce additional biases (Giorgi, 2006; Lucarini et al., 2007a). Moreover, dynamical downscaling still does not provide information at station scale and may need to be downscaled further. The use of high-resolution hydrological models taking input from the GCMs and the RCMs also needs a robust calibration/validation process and is prone to add an additional layer of uncertainty due to the lack of sufficient observational data at the required spatio-temporal scales. On the other hand, statistical downscaling techniques are less computationally expensive, but uncertainties emerge from the fact that no universal technique exists for linking predictands and predictors, and that the training sets can be uncertain or inadequate, especially in the regions where the observational record is short or even missing.

ESDD
4, 109–177, 2013

The spatial analogue approach depends upon the tele-connections between the present climate of one geographical location with the future climate of another region (Parry et al., 1988; Arnell et al., 1996) with temporal analogue techniques based on the historical and the paleoclimatic records to generate the future scenarios (Krasovskania and Gottschalk, 1992; Knox, 1993).

The direct use of GCM output data may include the computation of a basin-wide integration of the hydrological quantities as simulated by the GCMs under the given forcing. The runoff routing routines can be further used to translate runoff into synthetic discharge, to be comparable with the observational record (Arora and Boer, 2001; Nohara et al., 2006). The analysis of the representation of the hydrological cycle in GCMs suggests that intra-model discrepancies and inconsistencies exist at a spatio-temporal scale. These result from differences in the representation of the large scale circulation, of the ocean-atmosphere interaction, in the representation of orography, and in the description of the exchanges of water in liquid, solid and gaseous form between soil and atmosphere (Lucarini, 2007b, 2008; Previdi and Liepert, 2007; Liepert and Previdi, 2012). The skills and limitations for the above given three main methods are discussed in detail by Chong-yu (1999) and Arora and Boer (1999, 2001).

The GCMs, despite of their coarse resolution and the structural differences, are still considered one of the few physically based tools to investigate the response of GHG forcing on various climate system components such as the hydrological cycle. The limitations of the coarse horizontal resolution of these models are less severe when considering basin-wide integrated quantities, especially for the large river basins encompassing a reasonable number of grid cells (Lucarini et al., 2008). Hagemann et al. (2006) has found comparably small effect of increase in the horizontal resolution than in the vertical resolution while analyzing the performance of ECHAM5 model in representing the hydrological cycle of the global river basins. In this study, we take the pragmatic approach of directly using the output of a set of coupled GCMs with the goal to perform an auditing and the verification procedure for their representation of the hydrological cycle over the four South and Southeast Asian river basins in the XX century

Discussion Paper | Discussion Paper | Discussion Paper | Discussion Paper |
ESDD
4, 109–177, 2013
Hydrological cycle over south and southeast Asian river basins
S. Hasson et al.

and also to understand the range of climate projections in the later part of the XXI and XXII centuries.

3.2 Data sets

Our analysis is based on the data relative to the last 40 yr of the XX century climate reconstructions and of the XXI and XXII centuries' climate projections based on the SRES A1B scenario runs of the AOGCMs (see Table 2 for details) included in the PCMDI/CMIP3 project (http://www-pcmdi.llnl.gov/). We have considered monthly values of the relevant climatic variables such as Total Runoff (R), Precipitation (P) and Evaporation (E). Evaporative fields have been reconstructed from the surface upward latent heat fluxes. We have restricted our investigation to the GCMs providing the complete datasets for R, P, and E for the last 40 yr of all centuries considered. We remind that SRES A1B scenario runs correspond to a ramp-up of CO_2 concentration up to 720 ppm in 2100, with immediate stabilization of CO_2 concentration afterwards. Moreover, in order to understand the degree of realism of climate models in the reconstruction of the XX century climate, we have considered the historical XX century discharges (D) for all the rivers at either the last or near-to-sea gauging stations (Indus at Kotri, Ganges at Hardinge Birdge, Brahmaputra at Bahadurabad, and Mekong at Pakse) depending on the data availability. The discharge data for the Indus is collected from the Water and Power Development Authority (WAPDA), Pakistan, for the Ganges and the Brahmaputra from Jian et al. (2009), and for the Mekong River from Dia and Trenberth (2002).

3.3 Theoretical framework

Assuming that water storage in liquid and solid form is negligible in the column comprising a soil layer and the atmosphere aloft when long-term averages are considered (Peixoto and Oort, 1992; Karim and Veizer, 2002), at any point of the land surface, the fields P, E and R satisfy the balance equation:

ESDD
4, 109–177, 2013

$$\langle P\rangle_t - \langle E\rangle_t \approx \langle R\rangle_t \approx \langle \nabla_H \cdot \boldsymbol{Q}\rangle_t \tag{1}$$

where the subscript t denotes the temporal average, and $\nabla_H \cdot \boldsymbol{Q}$ is the divergence of water in the atmospheric column. Spatially integrating Eq. (1) over an area A of the river basin, the form of hydrological balance becomes:

$$\int_A \mathrm{d}x\,\mathrm{d}y\,(\langle P\rangle_t - \langle E\rangle_t) - \int_A \mathrm{d}x\,\mathrm{d}y\,\langle B\rangle_t \approx -\int_A \mathrm{d}x\,\mathrm{d}y\,\langle \nabla_H \cdot \boldsymbol{Q}\rangle_t \approx \int_A \mathrm{d}x\,\mathrm{d}y\,\langle R\rangle_t \approx \langle D\rangle_t \tag{2}$$

where B is the net balance and D is the observed discharge into the sea. Further details regarding the method and its suitability are discussed in detail by Lucarini et al. (2008). The equation is satisfied for the short term storages as the average time of water in the atmosphere is roughly 10 days, whereas routing time in the channels, snow accumulation and the groundwater storages range from month(s) to a season. Equations (1) and (2) provide an excellent approximation for describing the hydrological balance of a river basin if $t \geq 1$ yr under the assumption that the glaciers present in the basin observe negligible change in their inter-annual mass balance and are in somewhat stable conditions, or if the glaciers' mass balance gives minor corrections to the overall hydrological cycle. A small overall change in the glaciers' mass balance is observed in the Karakoram region (Scherler et al., 2011), which is relevant for the Indus River. A negative trend in the glaciers' mass is instead reported in the central and eastern portion of the HKH, but the overall correction due to this effect is expected to be small for the Ganges, Brahmaputra and Mekong basins, because of the fact that these rivers have, in any case, relatively small contribution from the snow and ice melt. Therefore, Eq. (2) is appropriate for our case studies.

Yearly time series of the spatially integrated four variables (P, E, $B = P - E$ and R) are computed for the considered time spans of 40 yr:

$$\overline{\beta}_i = \int_A \mathrm{d}x\,\mathrm{d}y\,\langle \beta\rangle_i \tag{3}$$

ESDD
4, 109–177, 2013

Hydrological cycle over south and southeast Asian river basins

S. Hasson et al.

where β_i, $i = 1, ..., 4$ corresponds to each of the four variables mentioned above, and A denotes the area of each considered river basin. The long-term averages and standard deviation of the yearly values are computed using Eqs. (4) and (5).

$$\mu\left(\overline{\beta}_i\right) = \frac{1}{40}\sum_{i=1}^{40}\overline{\beta}_i \tag{4}$$

$$\sigma\left(\overline{\beta}_i\right) = \sqrt{\left[\frac{1}{39}\sum_{i=1}^{40}\left(\overline{\beta}_i - \mu\left(\overline{\beta}_i\right)\right)^2\right]} \tag{5}$$

3.4 Data manipulation

The mean annual time series of all the relevant variables defined in the gridded domain of the climate models are computed using Voronoi or Thiessen tessellation method (Okabe et al., 2000) in the GrADS (Grid Analysis and Display System) and the GIS environment. The Thiessen tessellation method has been selected to avoid any kind of interpolation scheme, which may prevent the accurate computation of the volumetric quantities, usually along the perimeter of the study basin. The output has been projected to UTM (Universal Transverse Mercator) projection according to the central zone of each river basin covering relatively the maximum of the basin area. For the grid cells partially lying inside/outside the basin, only the fraction of area inside the basin has been considered to prevent water loss/gain. In this way, basin-wide integrated quantities are computed accurately. Similarly, the inconsistency between the land-sea mask given by GCMs and the basin boundaries exists due to the fact that each GCM has its own resolution and basin boundary is extracted using net accumulation from the areas present within a basin. The degree of difference is usually high for the coarse resolution GCM datasets. So any grid cell partially lying inside/outside the basin at the coastline must be checked how it is treated in the land-sea mask of the particular GCM. Usually these cells are considered as a sea cell and may or may not have a high precipitation rate, but indeed feature high evaporation and zero or missing runoff quantity.

ESDD
4, 109–177, 2013

Including such cells in the computation can introduce inaccuracies and significantly bias the computed water budget. So depending on the particular GCM and its land-sea mask, basin-wide quantities require a careful post-processing. The adapted approach fits well for each model having different grid resolutions.

3.5 Implications in assessing the water balance

Our analysis is based on the output from various CMIP3 GCMs. To synthesize the output of multi-models, a common approach of the ensemble mean and its spread is considered as the arithmetic mean and its standard deviation (Houghton et al., 2001). The approach was originally developed for the seasonal forecasting (Harrison et al., 1999) and found superior to each individual ensemble member (Fritsch et al., 2000). Giorgi and Mearns (2002) weighted the multi-model ensemble according to the performance of each participating GCM for the present climate to get reliable projections. However, a problem exists when considering the climate models' output as an ensemble members due to multiple reasons as discussed in detail by Lucarini et al. (2008) and Liepert and Previdi (2012) and are summarized here: (i) there is no way to correctly assign weights to climate models in terms of their quality due to huge inter-model structural differences; (ii) climate models' output do not form a sample from any well-defined probability distribution. Moreover, GCMs feature systematic spatio-temporal biases as discussed earlier. Therefore, taking the ensemble mean as the representative output from the multi-model simulations hides or cancels these biases than quantify them. These ensemble-mean based estimates can therefore be misleading for the impact assessment studies and consequently their use in the future planning becomes questionable. The study shows in the later section that how the models differ quantitatively as well as qualitatively with each other and that under such circumstances their ensemble mean are not realistically representative of the whole dataset. The ensemble shown in the results are therefore purely indicative.

ESDD
4, 109–177, 2013

4 Results

The results of our analysis are presented in two parts. In the first part, the skill of GCMs against all the relevant hydrological quantities and for the study basins is shown for the historical climate (1961–2000). This provides realization about the performance of the GCMs in representing the basin-scale hydrological cycle over the region and that how reliable their estimated future changes would be. Then, in the second part, the changes in the future climates of the XXI and XXII centuries with respect to the historical climate are presented for the same hydrological quantities. These hydrological quantities are the annual means and their variability for water balance ($B = P - E$), strength of the hydrological cycle ($H = P + E$), and the relationships between precipitation and the evaporation and between the water balance and the observed discharge.

4.1 Present climate

4.1.1 Water balance

The water balance is an important part of the river hydrology. The significant changes in the water balance of the river basins in terms of the timing and the magnitude can greatly influence the balance between the supplies and the demands and also the feedback to the hydrological cycle and the regional climate. For example, any inconsistency of 100 mm yr^{-1} in the water balance corresponds to the inconsistency of 7.2 Wm^{-2} in the energy balance of the atmosphere (Lucarini et al., 2008). Here, we present the mean annual water balance estimates for each basin and discuss their realism against the respective observed mean discharges. Also, we discuss the inter-model consistency for the computed mean annual water balance and its inter-annual variability among the models.

ESDD
4, 109–177, 2013

Indus basin

Figure 2a shows the scatterplot of mean annual water balance against its inter-annual variability for the Indus basin. Almost all the models vary on an inter-annual variability scale ranging between 30–70 mm yr^{-1}, with the four models (CNRM3.0, ECHAM5, HADGEM1 and IPSLCM4) suggesting a relatively high interval. Similarly, models are not consistent with each other for their mean estimates of the water balance. All models overestimate the mean water balance for the basin except PCM which shows the lowest value of about 10 mm yr^{-1}. CNRM model shows the highest value of almost 330 mm yr^{-1}, whereas the so-called ensemble mean is at 150 mm yr^{-1} with only the HADGEM1 close to it. However, the cluster of six models (CSIRO3.0, IPSL-CM4, HADCM3, INMCM, ECHO-G and CGCM2.3.2) around 70–100 mm yr^{-1} is relatively close to the observed mean annual discharge of almost 30 mm yr^{-1} for the Indus River. The large inter-model variability in mean is due to the wet bias in most of the models. There is a positive correlation between the mean annual water balance and its inter-annual variability within two different model sets like HADGEM1, ECHAM5 and CGCM2.3.2, as well as CNRM3.0, GFDL2.0, GISS-AOM and MIROC-HIRES as shown in the figure.

Ganges basin

Models neither agree for the mean annual water balance nor for its inter-annual variability (Fig. 2b). The inter-annual variability among the models ranges between 50–150 mm yr^{-1} approximately with a cluster of six models (CGCM2.3.2, GISS-AOM, HADCM3, CSIRO3.0, PCM and ECHO-G) around 60 mm yr^{-1}, and the five models (CNRM, MIROC-HIRES, HADGEM1, INMCM and IPSL-CM4) around 100 mm yr^{-1}. For the mean annual water balance, five models (HADCM3, CSIRO3.0, PCM, CGCM2.3.2 and ECHO-G) cluster around 200 mm yr^{-1}. The so called ensemble is around 260 mm yr^{-1} while the observed mean discharge is almost 350 mm yr^{-1}. HADCM3 and GISS-AOM are close to the ensemble mean. On the other hand, only GISS-AOM is

ESDD
4, 109–177, 2013

close to the mean observed value. Most of the models underestimate the water balance for the Ganges basin. The most important finding is the behavior of IPSL-CM4 and INMCM models, as both show a negative mean annual water balance. This case suggests the high evaporation, relatively low precipitation and no runoff in the semi-arid or the arid parts of the basin. In these parts, the computed water balance may be unphysical because of the model errors and their inability to explain the hydro-meteorological conditions in these areas. These unrealistic values can negatively influence the basin wide computed water balance as in the case of present study.

Brahmaputra basin

The inter-annual variability of the water balance shows good inter-model agreement as most of the models cluster around 100 mm yr^{-1} except two models (ECHAM5 and GFDL2.0) which show higher inter-annual variability (Fig. 3a). However, the overall spread of the inter-annual variability is large (i.e. 50–270 mm yr^{-1}). For the mean annual water balance, figure shows that again two models IPSL-CM4 and INMCM perform unrealistically as in case of the Ganges basin, suggesting almost no water balance for the Brahmaputra basin. ECHO-G also suggests very low water balance. ECHAM5 shows the highest value of above than 1600 mm yr^{-1}. A cluster of four models (CGCM2.3.2, CSIRO3.0, PCM and CNRM) is around 500 mm yr^{-1}. The mean observed discharge is approximately 1200 mm yr^{-1} however no single model is close to it. Two models (HADCM3 and GFDL2.0) are close to the so called ensemble which is around 740 mm yr^{-1}. It is clear from the figure that there are large differences between the observed and the so called ensemble values and also that all the models underestimate the water balance for the Brahmaputra basin as compared to the observed value of 1200 mm yr^{-1}.

Discussion Paper | Discussion Paper | Discussion Paper | Discussion Paper |

ESDD
4, 109–177, 2013

Hydrological cycle over south and southeast Asian river basins

S. Hasson et al.

Mekong basin

Figure 3b shows that most of the models agree on the inter-annual variability of the water balance roughly around 100 mm yr^{-1} except the five models (GISS-AOM, ECHAM5, PCM, GFDL2.0 and HADGEM1). The inter-annual variability spread is between 50–150 mm yr^{-1}. The mean annual water balance ranges from 200 to 830 mm yr^{-1} among four models (PCM, INMCM, GFDL2.0 and MIROC-HIRES) respectively. Only the five models do agree with each other regarding the mean annual water balance, with an approximate value of 460 mm yr^{-1} which is also close the so-called ensemble water balance. The mean observed discharge is around 650 mm yr^{-1} and only HADGEM1 and CGCM2.3.2 models are close to it. The results show that most of the models underestimate the water balance for the Mekong basin.

Here, we need to clarify that the models show large spread for the mean annual water balance for each basin. It is also the case that all the models participating in the analysis do not suggest a uniform response either of the underestimation or of the overestimation of the water balance for each basin as compared to their mean observed value. Under such circumstances, we see that the ensemble mean values do not realistically represent the models' performance in terms of the verification of the water balance quantity. Therefore, as discussed in previous sections, the interpretation of the models results still require careful thought to get the reliable information while the exclusive use of ensemble quantities may produce misleading conclusions. However, the qualitative analysis presents a general picture that most of the models suggest overestimation of the mean water balance quantity for the Indus basin, whereas those suggest underestimation of the same for all three rest of the basins.

4.1.2 Strength of hydrological cycle

The results of the mean annual strength of the hydrological cycle, calculated as $H = P + E$ for the historical climate of XX century (1961–2000) are presented here for all the four study basins. Also, the precipitation and the evaporation quantities are

ESDD
4, 109–177, 2013

plotted against each other to explore their possible influence on the strength of the hydrological cycle and are discussed in detail.

Indus basin

Figure 4a shows that there is a weak inter-model agreement for the mean annual strength of the hydrological cycle (between 500–1570 mm yr^{-1}) and its inter-annual variability (between 70–120 mm yr^{-1}). CNRM model suggests highest value around 1570 mm yr^{-1}. A relatively better inter-model agreement is found among the four models (INMCM, CSIRO3.0, CGCM2.3.2 and ECHO-G) around 550 mm yr^{-1}, and then other eight models (GISS-AOM, HADCM3.0, HADGEM1, GFDL2.0, PCM, MIROC-HIRES, ECHAM5 and IPSL-CM4) around 750 mm yr^{-1} which is quite close to the ensemble strength of the hydrological cycle for the Indus Basin. This ensemble value provides misleading information as it is heavily biased by the extraordinary value of the CNRM model. The minimum strength of the hydrological cycle for the Indus Basin is suggested by the CSIRO3.0 model around 450 mm yr^{-1}.

It is noted that CNRM model suggests quite high precipitation and relatively low evaporation. In contrast to this, PCM model suggests a minimum positive water balance with evaporation relatively closer to the precipitation. This is why CRNM shows the highest strength, but PCM does not show the lowest. This further emphasizes the fact that the ratio of the precipitation to the evaporation is different for each model. Therefore, it is necessary to look into these ratios to have a realistic sense of the strength of the hydrological cycle over the basin. In Fig. 4b we have shown the scatter plot of the precipitation against the evaporation to assess their individual contribution to the strength of the hydrological cycle. The ratios between precipitation and evaporation are different among the models and are usually greater or equal to one. All models are in the range of 300–600 mm yr^{-1} for precipitation against the range of 200–400 mm yr^{-1} for evaporation with modestly depicting less variability and high agreement for the water balance, except CNRM model which may be considered as an outlier. There is a good agreement between the four models (ECHO-G, INMCM, CISRO3.0 and CGCM2.3.2)

ESDD
4, 109–177, 2013

at 350 mm yr^{-1}, and the three models (ECHAM5, GISS-AOM and MIROC-HIRES) at 450 mm yr^{-1}. PCM model, as discussed before, suggests almost the same amount of evaporation as the precipitation and therefore suggests a minimum water balance for the Indus Basin. Most of the models overestimate the Indus basin precipitation as compared to the observations.

Ganges basin

Figure 5a presents the strength of the hydrological cycle for the Ganges Basin. There is a weak inter-model agreement for the both, the mean annual strength of the hydrological cycle and its inter-annual variability which ranges approximately between 800–2400 mm yr^{-1} and between 100–230 mm yr^{-1} respectively. Three models (ECHAM5, HADGEM1 and PCM) suggest relatively high inter-annual variability, whereas GISS-AOM suggests a very low. For the mean annual strength of the hydrological cycle, three models (ECHAM5, MIROC-HIRES and CNRM) show a relatively high strength of it for the Ganges basin. The four models (GISS-AOM, GFDL2.0, HADGEM1 and PCM) are close to the ensemble strength of the hydrological cycle which is around 1400 mm yr^{-1}. However, as obvious from the figure shown, the ensemble is highly influenced by the heavy contributions from ECHAM5, MIROC-HIRES and CNRM models. IPSL-CM4 suggests the weakest hydrological cycle at 800 mm yr^{-1}.

The relative high strength of the hydrological cycle for the Ganges Basin by three models (CNRM, ECHAM5, and MIROC-HIRES) is mainly due to their high precipitation and relatively low evaporation as shown in Fig. 5b. For CNRM, the precipitation is almost twice as large as its evaporation. CGCM2.3.2 and ECHO-G also have fewer differences between the suggested precipitation and the evaporation for the Ganges Basin. One more interesting fact found within the Ganges Basin is that INMCM and IPSL-CM4 suggest evaporation higher than the precipitation, presenting not only the minimum but also the negative water balance for the basin. These unrealistic results ($P - E < 0$) are another shortcoming of the climate models especially over the semi-arid

ESDD
4, 109–177, 2013

or arid parts of the basins and can result in an inaccurate assessment of the basin-wide water balances providing false estimates. Most of the models underestimate the Ganges basin precipitation as compared to the mean observed precipitation. However, it is noted that most of the models also agree well on the fact that the Ganges is relatively wetter basin than the Indus Basin. With few exceptions (CNRM for Indus and CGCM2.3.2 and IPSI-CM4 for Ganges) all models suggest the strength of the hydrological cycle for Indus less than 1000 mm yr^{-1} whereas for the Ganges greater than 1000 mm yr^{-1}.

Brahmaputra basin

Figure 6a shows that there is a large spread of inter-annual variability (between 90–270 mm yr^{-1}) among the models for the strength of the hydrological cycle. ECHAM5 suggests the highest inter-annual variability while the lowest variability is suggested by CGCM2.3.2. There exists a weak agreement among most of the models for the inter-annual variability of the strength of the hydrological cycle which is around 120 mm yr^{-1}. For the mean strength of the hydrological cycle, a good inter-model agreement is found among the cluster of five models (HADCM3, CGCM2.3.2, CNRM, GFDL2.0 and CSIRO3.0) which is around 2000 mm yr^{-1} with relatively low inter-annual variability. Again, we are of the view that the ensemble value, although close to the cluster, is influenced by the extreme contribution from the models outside of the cluster. The overall spread of the mean strength of hydrological cycle is large and ranges between 1200–3750 mm yr^{-1} with ECHO-G at the minimum and GISS-AOM at the maximum. For the Brahmaputra, models again suggest an intensified hydrological cycle as compared to the Ganges, where most of the models are less than 1500 mm yr^{-1} while for the Brahmaputra most of the models are above 1500 mm yr^{-1}.

Figure 6b depicts that the big differences among the models for the strength of the hydrological cycle are generally attributed to the precipitation regime. The models showing higher precipitation suggest strong hydrological cycle, whereas the models showing relatively low precipitation suggest a weak hydrological cycle. Four models

ESDD

4, 109–177, 2013

Hydrological cycle over south and southeast Asian river basins

S. Hasson et al.

(INMCM, IPSL-CM4 and ECHO-G) also show relatively weak hydrological cycle and suggest their precipitation comparable to their evaporation. It is the case that all the models varying in their precipitation amounts are in good agreement for the evaporation which is evident by the consistent behavior of evaporation among most of the models (i.e. around 600 mm yr^{-1}). The six models (CNRM, CGCM2.3.2, CSIRO3.0, PCM, HADCM3 and GFDL2.0) show better agreement for the precipitation and evaporation, whereas three models (IPSL-CM4, INMCM and ECHO-G) underestimate the Brahmaputra precipitation and rest of the models overestimate the Brahmaputra precipitation.

Mekong basin

The models show a large spread of the inter-annual variability of the strength of hydrological cycle for the Mekong Basin which ranges between 80–220 mm yr^{-1} approximately (Fig. 7a). However, a good agreement exists between the four models (CNRM, CSIRO3.0, GFDL2.0 and HADGEM1) at around 170 mm yr^{-1} and between the five models (ECHAM5, ECHO-G, IPSL-CM4, HADCM3.0 and MIROC-HIRES) around 130 mm yr^{-1}. The mean strength of the hydrological cycle for the Mekong Basin varies from 2000 to 3160 mm yr^{-1} with only good agreement between the four models (IPSL-CM4, INMCM, PCM and CSIRO3.0). Two models (GISS-AOM and MIROC-HIRES) show relatively high strength of the hydrological cycle with its low inter-annual variability, whereas INMCM shows the weakest hydrological cycle and its highest inter-annual variability. The ensemble strength of the hydrological cycle of the basin is about 2480 mm yr^{-1}, and only two models (CNRM and HADCM3) approach it. It is clear from the figure that all of the models suggest a high strength in the hydrological cycle over the Mekong Basin (above than 2000 mm yr^{-1}), as compared to the Brahmaputra Basin (less than 2000 mm yr^{-1}), the Ganges Basin (less than 1500 mm yr^{-1}), and the Indus Basin (less than 1000 mm yr^{-1}).

The Fig. 7b shows that the large spread in the strength of the hydrological cycle of the Mekong basin is obviously associated with the large inter-model differences for both precipitation and the evaporation. The figure shows that there is a large spread for the both, the precipitation (1120–1900 mm yr^{-1}) and the evaporation (760–1400 mm yr^{-1}). Most of the models underestimate the Mekong precipitation as compared to the mean observed value of about 1650 mm yr^{-1}. Two models (INMCM and PCM) suggest the lowest precipitation for the basin, whereas MIROC-HIRES suggests the highest. Similarly, GFDL2.0 suggests lowest evaporation for the Mekong basin, whereas GISS-AOM suggests the highest.

For the inter-annual variability of the strength of the hydrological cycle, all models show a similar behavior of a weak agreement among each other. However, the range of this variability is more or less the same among all the basins except for the Indus Basin where variability is relatively low. Overall, the models show quite good agreement for the mean evaporation quantity for all the basins than for the precipitation quantity. The Brahmaputra Basin experiences the highest inter-model agreement for the evaporation, but the weak agreement for the precipitation. However, it is also found that the inter-model variability increases from Indus to Brahmaputra basin whereas the Mekong basin shows the inter-annual variability larger than the Indus and smaller than the Ganges and Brahmaputra basins. It is also the case that the most of the models, generally underestimate the precipitation for all the study basins as compared to their respective mean observations.

4.1.3 Runoff

Another criterion we have used to check the consistency of models with each other and with the observations is the comparison of their computed water balances against their simulated runoff quantities to see how precisely these models conserve the water. Conservation of water means that the computed water balance of the basin should be equal to the total runoff generated within the basin scale. Here, we have presented the comparison of the computed water balances against the simulated total runoff quantities (surface and sub-surface) for each basin and the results have been discussed in

ESDD
4, 109–177, 2013

terms of the inter-model agreement and their closeness to the mean observations. The mean observed values are given for each basin in the equivalent (mm yr^{-1}) units.

Indus basin

Figure 8a shows that although far from the observed mean discharge, most of the models show quite good agreement between their computed water balance and the simulated total runoff within their associated statistical uncertainties. PCM, though, performs well in terms of its water conservation but underestimate the water balance against the mean observed discharge suggesting quite low value around 10 mm yr^{-1}. Therefore, we consider PCM model as a dry model for Indus basin. Two models (CNRM and GISS-AOM) explain relatively higher water balances against their respective simulated runoff quantities. On the other hand, two models (IPSL-CM4 and INMCM) show opposite behavior suggesting higher simulated runoff as compared to their respective computed water balances.

Ganges basin

Figure 8b shows more surprising result as are discussed before in the water balance section that IPSL-CM4 and INMCM produce negative water balances for the Ganges Basin. This is the situation where over some parts of the basins these models calculate high evaporation as compared to precipitation and no runoff (surface and sub-surface runoff). These quantities further negatively influence the water balance for other humid parts of the basin. Again, there is no agreement between models' simulated runoff and the computed water balance with the mean observed discharge from the Ganges basin. However, most of the models suggest good agreement between their simulated runoff and the computed water balances. PCM suggesting slightly higher water balance whereas HADGEM1 suggesting slightly higher runoff are again close to the agreement.

ESDD
4, 109–177, 2013

Brahmaputra basin

Figure 9a shows That IPSL-CM4 and INMCM show almost no water balance and the lowest total runoff and so, suggest no agreement between these two quantities. Besides these two models, PCM shows a slightly lower simulated runoff value against the computed water balance. For all other models there is a strong agreement between the mean simulated total runoff and the computed water balances for the Brahmaputra basin. Again, no model is close to the observed discharge of the Brahmaputra River. Most of the models underestimate the water balance and the total runoff quantities

Mekong basin

Figure 9b shows that PCM has the lowest water balance as well as runoff, with the computed water balance slightly more than the simulated runoff. Three models (HADGEM1, INMCM and IPSL-CM4) have slightly low runoff as compared to their computed water balances. The rest of the models show good agreement between the two quantities at a basin scale. Only two models (CGCM2.3.2 and HADGEM1) are close to the observed discharge. However, again most of the models underestimate the water balance and the total runoff quantities.

4.2 Projected changes: XXI and XXII centuries

Though the GCMs' performance in simulating the hydrological quantities is not satisfactory against the observations, however, there is a consistent behavior among models between their computed water balances and the simulated total runoff. Therefore, it is plausible to investigate, what future changes in the hydrological cycle are suggested by these models. For this, we have presented here the future changes in the hydrological quantities for the later part of the XXI (13 models) and the XXII (10 models) centuries relative to the corresponding time span of the XX century for IPCC SRES A1B scenario and have discussed here.

ESDD
4, 109–177, 2013

Indus basin

Inter-annual variability in the computed water balance does not change significantly throughout the XXI and XXII centuries for the Indus Basin (not shown here). For the mean annual computed water balance, only five models (HADCM3, HADGEM1, PCM, CNRM and GISS-AOM) suggest a positive change in the water balance for the XXI century, whereas majority of the models suggest a negative change. Similarly, for the XXII century, only four models (HADCM3, HADGEM1, CSIRO3.0 and IPSL-CM4) show a positive change while the rest of the models show a negative change which is relatively high as compared to the XXI century change.

Most of the models suggest a positive change in the strength of the hydrological cycle for the XXI century (Fig. 10). However, the three models (GFDL2.0. ECHAM5 and INMCM) suggest a negative change and the two models (IPSL-CM4 and HADGEM1) suggest almost no change. For the XXII century, except three models (ECHAM5, GFDL2.0 and HADGEM1), all models show even pronounced positive change as compared to the XXI century change. The reason for the negative future water balances suggested by ECHAM5 and GFDL2.0 models for Indus basin is due to higher negative change suggested for precipitation than for the evaporation (Fig. 11). Likewise, for INMCM it is attributed to the negative change in precipitation only for the XXI century and the relative higher negative change in the precipitation for the XXII century. IPSL-CM4 suggests a negative change in precipitation but a positive change in evaporation for the XXI century. The rest of the models suggest a positive change in both, the precipitation and the evaporation, although the ratios between these two quantities are different among the models. On the other hand, three models (CGCM2.3.2, CSIRO3.0 and ECHO-G) for the XXI century and three models (CNRM3.0, ECHO-G and CGCM2.3.2) for the XXII century show higher positive change in evaporation relative to the precipitation. MIROC-HIRES shows almost the same positive change for both evaporation and precipitation in the XXI century.

ESDD
4, 109–177, 2013

Ganges basin

Figure 12 shows that the three models (ECHAM5, IPSL-CM4 and INMCM) suggest a negative change for the mean annual water balance of the Ganges Basin as well as a decrease in its variability for both XXI and XXII centuries. CSIRO3.0 shows a slight negative change in the mean water balance for the XXI and XXII centuries, whereas decrease in its variability for XXI and no change in it for the XXII century. On the other hand, PCM shows an increase in the mean annual water balance and decrease in its variability only for the XXI century. Most of the models suggest increase in the mean annual water balance as well as in its variability for the Ganges basin for the XXI and XXII centuries.

Figure 13 shows the strength of the hydrological cycle for the Ganges Basin. Almost all models show a positive or no change in the strength of the hydrological cycle for the Ganges Basin for the XXI and XXII centuries, except INMCM and IPSL-CM4. We already discussed that these two models do not perform well over the Ganges basin. CSIRO3.0 does not suggest any change for both XXI and XXII centuries, whereas ECHAM5 does not suggest any change for the XXI century only. The rest of the models suggest positive change in the strength of the hydrological cycle for the Ganges basin. Figure 14 shows the comparison of changes in precipitation and evaporation for the Ganges Basin. It is clear from the figure that the main reason for the negative change in the water balances and the strength of the hydrological cycle suggested by IPSL-CM4 is attributed to the negative change in both precipitation and evaporation for both centuries. For INMCM, however, it is associated with the negative change in precipitation and positive change in evaporation for the XXI century and the negative change in both quantities for the XXII century. Also, the negative changes in the mean water balance and no change in the strength of the hydrological cycle associated with the ECHAM5 and CSIRO3.0 for the XXI century are attributed to negative and positive changes in the precipitation and evaporation respectively for ECHAM5 and the negative change in the precipitation only for CSIRO3.0. For the XXII century, these are

ESDD
4, 109–177, 2013

associated with the slight positive change in evaporation for CSIRO3.0 and a higher positive change in evaporation relative to the precipitation for the ECHAM5 model.

The positive change in the strength of the hydrological cycle as well as water balance suggested by HADGEM1 and GFDL2.0 for the Ganges Basin in the XXI and XXII centuries is attributed to a relatively high positive change in precipitation than the negative change in the evaporation. For the rest of the models, which show a positive change in the strength of the hydrological cycle and the water balance, this is due to an increase in both precipitation and evaporation. The ratio between projected change in evaporation and projected change in precipitation is different for each model. Although, there is no uniform behavior of GCMs' response for the changes in water balance and strength of the hydrological cycle for the Ganges Basin, however, most of the models agree in suggesting a positive change in water balance for the XXI century and the higher magnitude of its change for the XXII century, whereas for the strength of the hydrological cycle almost all models agree on a positive or no change for both centuries. The positive change in the strength of the hydrological cycle and the water balance for the Ganges Basin shown by some models is due to a higher increase in precipitation than evaporation.

Brahmaputra basin

Figure 15 shows that there is quite good inter-model agreement for almost no change in the inter-annual variability of water balance for the XXI century except ECHAM5 which suggests a decrease, and the four models (GISS-AOM, HADGEM1, MIROC-HIRES and GFDL2.0) which suggest an increase. For the XXII century, most of the models suggest an increase in the inter-annual variability but the inter-model differences are large. Only CNRM suggests no change in the inter-annual variability, whereas three models (ECHAM5, IPSL-CM4 and INMCM) suggest a decrease. For the mean annual water balance, most of the models agree for a positive change. Only four models (IPSL-CM4, INMCM, ECHAM5 and CSIRO3.0) suggest a negative change in the mean annual water balance for both XXI and XXII centuries.

ESDD
4, 109–177, 2013

The strength of the hydrological cycle for the Brahmaputra Basin is shown in the Fig. 16. Only IPSL-CM4 suggests negative change, whereas three models (ECHAM5, INMCM and CSIRO3.0) suggest almost no change for the XXI and XXII centuries. The rest of the models agree on an increase in the strength of the hydrological cycle. Figure 18 further investigates these changes in in terms of changes in the precipitation and the evaporation. It is found that the negative change in the water balance and in the strength of hydrological cycle suggested by IPSL-CM4 is due to the negative change in both precipitation and evaporation for the XXI and XXII centuries. For ECHAM5, the negative change in the water balance and no change in the strength of the hydrological cycle are due to the negative and positive changes in the precipitation and the evaporation respectively. Similarly, the negative projected change for water balance and no change in the strength of the hydrological cycle for CSIRO3.0 are mainly due to no change in precipitation and an increase in evaporation for the XXI century, and a relatively higher increase in evaporation than increase in precipitation for the XXII century. In contrast to this, INMCM projects a negative change for the water balance while no change in the strength of the hydrological cycle which is mainly due to the relatively higher increase in evaporation than in precipitation for the XXI century, and a decrease in precipitation only for the XXII century. For the Brahmaputra Basin, there is quite good agreement between models regarding the positive or no change in evaporation. The rest of the models show an increase in the strength of the hydrological cycle as well as in the water balance. These increases are mainly associated with the higher increase in the precipitation than in the evaporation.

Mekong basin

All models suggest an increase in the inter-annual variability of the water balance for the Mekong Basin with modest agreement, except two models (ECHO-G and HADGEM1) which suggest decrease and two models (INMCM and HADCM3) which suggest no change for the XXI century (Fig. 18). Similarly, most of the models suggest increase in the inter-annual variability of water balance for the XXII century as well

ESDD
4, 109–177, 2013

except two models (ECHO-G and CSIRO3.0) suggesting a negative change whereas two models (INMCM and CGCM2.3.2) suggesting almost no change. Regarding the mean annual water balance for the Mekong Basin, there is again high agreement between models for its projected increase with HADGEM1 showing the highest while IPSL-CM4 suggesting almost no change. No model suggests a decrease in the mean annual water balance for the Mekong Basin. For the XXII century, only INMCM shows almost no change for the mean annual water balance whereas only IPSL-CM4 shows a negative change in the mean water balance and a positive change in its variability. Two models (ECHO-G and CSIRO3.0) show a decrease in the inter-annual variability of the water balance but an increase in the mean annual water balance.

The rest of the models show an increase in both the mean annual water balance and its variability. Figure 19 shows the changes in the strength of the hydrological cycle for the XXI and XXII centuries. Three models (IPSL-CM4, CSIRO3.0 and GFDL2.0) suggest no change in the strength of the hydrological cycle by the XXI century, whereas the rest of all models suggest an increase. For the XXII century, two models (IPSL-CM4 and HADGEM1) show a decrease in the strength of the hydrological cycle, three models (CSIRO3.0, INMCM and GFDL2.0) suggest no change, whereas the rest of the models suggest a positive change. It is noted that only few models agree with each other for the magnitude of change.

Figure 20 shows the projected mean precipitation and the evaporation for the XXI and XXII centuries. For IPSL-CM4, there is a negative projected change in both precipitation and evaporation for the XXI and XXII centuries. Five models (GFDL2.0, CSIRO3.0, ECHO-G, HADCM3 and HADGEM1) show a positive change in precipitation and a slight negative change in the evaporation for the XXI century and the five models (HADGEM1, HADCM3, CSIRO3.0, ECHO-G and GFDL2.0) show a positive change in precipitation with almost no change in evaporation. For the XXII century, INMCM suggest a negative change in precipitation and almost no change in the evaporation. The rest of the models which show an increase in the both precipitation and the evaporation,

ESDD
4, 109–177, 2013

agree on the fact that this increase is relatively higher for the precipitation than for the evaporation.

5 Discussions and conclusions

In this study we have analyzed how the hydrological cycle of four major South and Southeast Asian rivers (Indus, Ganges, Brahmaputra and Mekong) are represented by CMIP3 GCMs simulations for the period 1961–2000 (present-day climate) and what future changes are foreseen by these models for the periods 2061–2100 and 2161–2200 under an intermediate warming scenario (IPCC SRES A1B scenario). We have focused on the basin integrated values of water balance, runoff, precipitation, and evaporation. The focus here has been on assessing how the climate models manage to simulate annual mean conditions over such periods. The inter-model agreement for the simulated hydrological quantities and their relevance to the mean observation is also assessed. Our results presented here further augment the need to decompose the analysis to study the representation of hydrological cycle and its expected future changes at the inter-seasonal timescale.

5.1 Models performance for the present-day climate

Although CMIP3 models show an appreciable spread in simulating the quantities related to the hydrological cycle for all four river basins, some common trends are evident. First, CMIP3 models clearly show the positive gradient of the precipitation and the strength of the hydrological cycle from the Indus to the Mekong basin. This informs us that in spite of model uncertainties in predicting monsoon rainfall they still capture some common observed properties.

Another interesting feature is the qualitative different behavior of evaporation and precipitation, with the Indus showing some remarkable differences when compared to the other three river basins. The basin-integrated precipitation ranges in wide intervals

ESDD
4, 109–177, 2013

for the Ganges (400–1400 mm yr^{-1}), Brahmaputra (500–2500 mm yr^{-1}) and Mekong (1000–2000 mm yr^{-1}), whereas for the Indus such range is considerably smaller in absolute and relative terms (300–500 mm yr^{-1}) and comparable with the inter-model evaporation range, which instead is relatively narrow for all river basins. Such differences between the Indus, Ganges, Brahmaputra and Mekong basins point out a basic difference in the precipitation regimes associated with such river basins. The Ganges, Brahmaputra and Mekong basins receive precipitation water mainly because of the summer monsoon since their basins are centrally located with respect to the area affected by monsoon precipitations (Annamalai et al., 2007). The observed records show that the average precipitations over the basin of the Indus instead come, more or less in equal proportion, from the summer monsoon and partially from the winter snowfalls over the large Hindu kush-Karakoram mountains, and due to the extra tropical cyclones originating over the Caspian and the Mediterranean sea at the east-most extremity of the Atlantic and Mediterranean storm tracks (Hodges et al., 2003; Bengtsson et al., 2007). The Indus Basin area, located at the border of these two main large scale circulations, is therefore characterized by a non-trivial meteorology, posing a challenge to climate models in simulating them realistically.

Differences in the precipitation regimes also emerge in the runoff model simulations. Most of the models underestimate the precipitation for all the four study basins. This misrepresentation of the precipitation regime by CMIP3 models can partly be associated with their spatial bias of the Indian summer monsoon precipitation maxima which is shifted towards equator at 12° N (Lin et al., 2008). Also, almost all the models (except one, PCM) tend to overestimate the Indus basin water balance whereas for the Ganges (8 vs. 5), Brahmaputra (9 vs. 4) and Mekong (9 vs. 4) river CMIP3 models either underestimate or overestimate it. Most of the models however, suggest the underestimation of the water balance for the Ganges, Brahmaputra and the Mekong basins and overestimate for the Indus basin. CMIP3 models show a remarkable uncertainty in simulating the hydrological cycle of these four major South and Southeast Asian rivers. This is inevitably linked to the capability of general circulation models in simulating realistically

ESDD
4, 109–177, 2013

the summer monsoon (Turner and Annamalai, 2012) and its variability, which is limited by model uncertainties and biases. A recent paper by Boos and Hurley (2012), for example, links an inaccurate representation of orography to a bias in the thermodynamic structure of the summer monsoon as represented by CMIP3 and CMIP5 models, and he shows that this is associated with ensemble-mean negative anomalies in precipitation over the Indian region. This is partially consistent with our results since, as explained, most of models tend to underestimate rainfall over the study basins.

As far as water balance is concerned, a large spread can be seen for all models and all basins and in particular for the Brahmaputra. The inter-annual variability of the mean water balance is also quite high among all the basins, however, the Indus Basin has relatively the lowest and the Brahmaputra has relatively the highest. Three models (CNRM, ECHAM5 and IPSL-CM4) have very large inter-annual water balance variability in the case of the Indus Basin, and ECHAM5 has the highest inter-annual variability for both Ganges and Brahmaputra basins. HADGEM1 exhibits the largest inter-annual variability for the Mekong Basin water balance. This inter-annual variability in the water balance is largely associated with the variability in the monsoon system. The main reason is the interaction of the mid-latitude circulation with the monsoon system over the study region as the westerly troughs can penetrate deeper and suppress the monsoon thermal contrast by the cold air advection over the monsoon dominated region and weakens the monsoon strength (Kripalani et al., 1997; Zickfeld et al., 2005). This interaction causes the monsoon onset delays and also the breaks. The resultant variability in the water balance brings severe implications of the extreme wet and droughts conditions in the region.

MIROC-HIRES shows relatively high precipitation values for all basins except the Indus. CNRM is unrealistically wet for the Indus, and PCM predicts a similar amount of evaporation and precipitation, that is to say a dry Indus. For the Ganges basin, again CNRM and MIROC-HIRES show the highest strength of the hydrological cycle, and INMCM and IPSL-CM4 the unrealistic negative water balances. For Brahmaputra, GISS-AOM, ECHAM5, MIROC-HIRES and HADGEM1 show a very strong hydrological

ESDD
4, 109–177, 2013

cycle due to high precipitations, whereas INMCM, IPSL-CM4 and ECHO-G have the lowest amount of precipitation. For the Mekong basin, GISS-AOM and MIROC-HIRES show the largest amounts of evaporation and the precipitation respectively, whereas INMCM shows the weakest hydrological cycle, with INMCM and PCM having the lowest precipitation-to-evaporation ratio and the river discharge.

In terms of consistency between mean annual quantities of water balance and simulated runoff, GISS-AOM, CNRM, IPSL-CM4 and INMCM suggest inconsistencies for the Indus basin, as the former two predict a water balance larger than the runoff, and the latter two the opposite. As far as the Ganges basin is concerned, IPSL-CM4 and INMCM have a negative water balance but a positive runoff, whereas in the case of the Brahmaputra River Basin these same two models are plainly inconsistent as they simulate practically a null water balance versus a non-zero but unrealistically small runoff. In spite of the large inter-model variability, some models however tend to cluster (e.g. annual mean water balance and its inter-annual variability). This is evident, for example, when we look at the mean water balance for all river basins and particularly in the case of the Brahmaputra and Mekong, with the ensemble mean not corresponding to any simulated point and/or cluster of points. We have seen before that the models do not show a uniform behavior for some of the hydrological quantities (underestimation/overestimation) and suggest large spreads with weak or no inter-model agreement. Therefore, we are of the view that considering the ensemble or arithmetic means of the relevant quantities for verification procedure neither owes any statistical value nor any practical significance. And that estimates relying on ensemble quantities can be quite misleading.

5.2 Future warming scenario

Analysis of the XXI and XXII century CMIP3 simulations show that there is a large variation in the spread of simulated hydrological quantities for all the four river basins, which prevents precise quantitative analysis. However, some general trends emerge from the models' inter-comparison analysis. This is generally in agreement with the

ESDD
4, 109–177, 2013

present knowledge of the effects of increased CO_2 levels in the South Asian summer monsoon (Cherchi et al., 2011; Turner and Annamalai, 2012), although understanding how the monsoon will change still poses a great challenge to the climate science community. Our analysis shows that the models generally suggest an increase in precipitation over all the study basins under the SRES A1B scenario throughout the XXI and XXII centuries. As we know that the large part of these study basins is under the influence of the monsoon system, so we can attribute this to the increase in the monsoon precipitation. This increase is associated with the increase in the thermal contrast between the Indian continent and the Indian Ocean and also with the increase in the atmosphere moisture content, though, monsoon circulation is suggested to be weaker under the warmer climates (May, 2002). But these increases in the precipitation do not necessarily correspond to the increases in the runoff or the water budget as the river basin may experience higher evapotranspiration, resulting in a runoff drop. However, our study shows that most of the models predicting an increase in precipitation, predict an increase in evaporation too, although of a minor magnitude. Furthermore, the increase in the strength of the hydrological cycle is mostly associated with an increase in the precipitation of the CMIP3 models.

According to CMIP3 projections, the Ganges, Brahmaputra and Mekong will experience an increased variability in their water balance, thus indicating a possible increase in the frequency of extreme events (dry and wet conditions). As discussed before, this is due to the weakening of monsoon due to cold air advection from westerly over monsoon season dominated region. The increase in inter-annual variability of the water balance implies that there would be high probability of the negative feedback from the mid-latitude circulations under the warmer climate. This issue will require more research since, in the light of recent extreme events in the area (e.g. the 2010 Pakistan flood) it is of high societal value. Going more into each specific case, no considerable change is found in the inter-annual variability of water balance for the Indus (range $\pm 20\,\mathrm{mm\,yr^{-1}}$ for the XXI century and similarly for the XXII century), with a robust agreement between models for the Indus basin. Most of the models suggest a negative change in the mean

ESDD
4, 109–177, 2013

water balance for both XXI and XXII centuries, although with a high inter-model spread. This is a remarkable difference with respect to the other three river basins, for which CMIP3 simulations foresee mainly an increase in the water balance.

A decrease in water balance is associated with an increase in precipitation smaller than evaporation in the case of CGCM2.3.2, CSIRO3.0 and ECHO-G models for the XXI century, whereas, as far as ECHAM5 and GFDL2.0 are concerned, this is explained by large precipitation negative anomalies larger in magnitude than the evaporation negative anomalies. Negative changes in precipitation and no changes in evaporation explain the decrease of the water balance of the INMCM model for the XXI century and the negative change in precipitation but positive change in evaporation in the case of IPSL-CM4 model for the XXI century. All other models predict a rise in the water balance and the strength of the hydrological cycle due to a growth in precipitation larger than the growth in evaporation.

Such contradictory results for the Indus basin are due to the fact that its water balance is determined by a more complex atmospheric circulation with both mid-latitude cyclones and summer monsoon which are roughly contributing equally. However, we cannot say conclusively that the suggested negative balance for Indus is whether associated with changes in the precipitation regime of the monsoon in summer, with the westerly winds in the winter or with the both. So, it is quite worthwhile to decompose the analysis further at the inter-seasonal scale to see first that how the hydrological cycle is represented at a seasonal time scale and then what factors are actually responsible for the future changes in the relevant hydrological quantities. Also an important role in future climate will be played also by the snowfall over the HKH glaciers, which are fed by winter mid-latitude cyclones, and by the effect of a warmer climate on such glaciers. In particular, in present day conditions, snowmelt and rainfall fluctuations are compensated by the glacier melt. At the moment, it is not clear how this will change in the future. Therefore, it is crucial to analyze correctly how the rainfall and the snowfall will change in the future in order to understand changes in the Indus basin hydrology. However, the compensation of monsoon rainfall to the glacier melt is challenging to analyze.

ESDD
4, 109–177, 2013

According to our present knowledge about the changes in the monsoon precipitation by the end of the XXI and XXII centuries, future response of glaciers to runoff is not very clear, especially for the Indus Basin which has a large portion of its discharge dependent on the glacier melt in addition to the snowmelt. The modeling study suggests a decrease in the runoff for the late spring and summer seasons after the period of rapid glacier melt (Immerzeel et al., 2010), which actually depends crucially on how much monsoon precipitation compensates the melt runoff under the warmer climate. In this regard, therefore, we suggest the similar analysis at the inter-seasonal scale.

Moving to the purely monsoonal basins, we have shown that CMIP3 models predict for the Ganges an increase in inter-annual variability, in most of the models by the XXI and XXII centuries, although there is no uniform response regarding changes in the water balance and in the strength of the hydrological cycle. However, in case of the water balance, most of the models agree on a positive change in the XXI century with a higher magnitude in the XXII century whereas, as far as the strength of the hydrological cycle is concerned, almost all models agree on a positive or no change for both centuries. Similarly, most of the models show an increase in the strength of the hydrological cycle and the water balance for the Brahmaputra Basin too, and no change in the inter-annual variability of water balance in the XXI century, but an increase for the XXII century. In both cases this is strongly related to the increase in monsoonal precipitation over the Indian region due to the effects of global warming on the monsoon circulation (Cherchi et al., 2011; Turner and Annamalai, 2012; Stowasser et al., 2007). Finally, also for the Mekong Basin, most of the models show an increase in the water balance, inter annual variability and the strength of hydrological cycle for the XXI and XXII centuries. However, there is a modest agreement between the most of the models on the water balance and its variability for the XXI century only, though, there is almost no agreement for the other hydrological quantities for the XXI and XXII centuries. Again we relate these changes, as in the case of the Ganges and Brahmaputra, to the enhancement of monsoonal precipitation as predicted by CMIP3 models under warmer climate.

ESDD
4, 109–177, 2013

As a future plan, we aim to delve into the dynamical mechanisms impacting the precipitation and the evaporation in this target area, by assessing the specific role of monsoonal and mid-latitude circulation structures. In this regard, the understanding of the hydro-climatology of the Indus and its variations in the context of climate change seem especially challenging and interesting. For this it is necessary to look at the seasonal variability for all the relevant quantities and additionally the temperature regimes over the region for the present and the future climates. Therefore, seasonal analysis is suggested as a natural successive in order to have a more detailed picture of the present and the future hydrological situation of the South and South East Asian region. Moreover, additional efforts will be directed at computing hydro-climatological indices such as the Standardized Precipitation Index (SPI) in this region for various GCMs and for various time frames covering the XX, XXI and XXII centuries. Finally, we aim at extending the present investigation to the CMIP5 models, whose outputs have been recently been made available, and test how GCMs performances and outputs have changed as result of about 5 yR of intense models' development.

Acknowledgements. The authors acknowledge the modeling groups, the Program for Climate Model Diagnosis and Inter-comparison (PCMDI) and the WCRP's Working Group on Coupled Modeling (WGCM) for their roles in making available the WCRP CMIP3 multi-model dataset. Support of this dataset is provided by the Office of Science, US Department of Energy. V. L. and S. P. acknowledge the support of the ERC Starting Investigator grant NAMASTE/Thermodynamics of the Climate System. SH acknowledge the support of BMBF, Germany's Bundle Project CLASH/Climate variability and landscape dynamics in Southeast-Tibet and the eastern Himalaya during the Late Holocene reconstructed from tree rings, soils and climate modeling. The authors also acknowledge the support from CliSAP/Cluster of excellence in the Integrated Climate System Analysis and Prediction. The authors also acknowledge Sabine Ehrenreich for her contribution in editing and improving the manuscript.

References

Annamalai, H., Hamilton, K., and Sperber, K. R.: The south-Asian summer monsoon and its relationship with ENSO in the IPCC AR4 simulations, J. Climate, 20, 1071–1092, 2007.

Arora, V. K. and Boer, G. J.: A variable velocity flow routing algorithm for GCMs, J. Geophys. Res., 104, 30965–30979, 1999.

Arora, V. K. and Boer, G. J.: Effects of simulated climate change on the hydrology of major river basins, J. Geophys. Res., 106, 3335–3348, 2001.

Arnell, N. W. and Reynard, N. S.: The effects of climate change due to global warming on river flows in Great Britain, J. Hydrol., 183, 397–424, 1996.

Archer, D. R. and Fowler, H. J.: Spatial and temporal variations in precipitation in the Upper Indus Basin, global teleconnections and hydrological implications, Hydrol. Earth Syst. Sci., 8, 47–61, doi:10.5194/hess-8-47-2004, 2004.

Bajracharya, S. R. and Shrestha, B.: The status of glaciers in the Hindu Kush-Himalayan region, ICIMOD, Kathmandu, 2011.

Bengtsson, L., Hodges, I. K., and Roeckner, E.: Storm tracks and climate change, J. Climate, 19, 3518–3542, 2007.

Bharati, L., Lacombe, G., Gurung, P., Jayakody, P., Hoanh, C. T., and Smakhtin, V.: The impacts of water infrastructure and climate change on the hydrology of the Upper Ganges River Basin, IWMI Research Report 142, International Water Management Institute, Colombo, Sri Lanka, p. 36, doi:10.5337/2011.210, 2011.

Boos, W. and Hurley, J.: Thermodynamic bias in the multi-model mean boreal summer monsoon, J. Climate, doi:10.1175/JCLI-D-12-00493.1, in press, 2012.

Cherchi, A., Alessandri, A., Masina, S., and Navarra, A.: Effects of increased CO_2 levels on Monsoons, Clim. Dynam., 37, 83–101, 2011.

Chong-yu, X.: From GCMs to river flow: a review of downscaling methods and hydrologic modelling approaches, Prog. Phys. Geogr., 23, 229–249, 1999

Center for International Earth Science Information Network (CIESIN)/Columbia University, and Centro Internacional de Agricultura Tropical (CIAT), Gridded Population of the World, Version 3 (GPWv3): Population Density Grid, Future Estimates, http://sedac.ciesin.columbia.edu/data/set/gpw-v3-population-density-future-estimates, last access: 23 December 2012, NASA Socioeconomic Data and Applications Center (SEDAC), Palisades, NY, 2005.

ESDD
4, 109–177, 2013

Hydrological cycle over south and southeast Asian river basins

S. Hasson et al.

Christensen, N. S., Wood, A. W., Voisin, N., Lettenmaier, D. P., and Palmer, R. N.: The effects of climate change on the hydrology and water resources of the Colorado River Basin, Climatic Change, 62, 337–363, 2004.

Dia, A. and Trenberth, K. E.: Estimates of Freshwater Discharge from Continents: Latitudinal and Seasonal Variations, J. Hydrometeorol., 3, 660–687, 2002.

Delworth, T. L., Broccoli, A. J., Rosati, A., Stouffer, R. J., Balaji, V., Beesley, J. A., Cooke, W. F., Dixon, K. W., Dunne, J., Dunne, K. A., Durachta, J. W., Findell, K. L., Ginoux, P., Gnanadesikan, A., Gordon, C. T., Griffies, S. M., Gudgel, R., Harrison, M. J., Held, I. M., Hemler, R. S., Horowitz, L. W., Klein, S. A., Knutson, T. R., Kushner, P. J., Langenhorst, A. R., Lee, H.-C., Lin, S.-J., Lu, J., Malyshev, S. L., Milly, P. C. D., Ramaswamy, V., Russell, J., Schwarzkopf, M. D., Shevliakova, E., Sirutis, J. J., Spelman, M. J., Stern, W. F., Winton, M., Wittenberg, A. T., Wyman, B., Zeng, F., and Zhang, R.: GFDL's CM2 global coupled climate models – Part 1: Formulation and simulation characteristics, J. Climate, 19, 643–674, 2005.

Eastham, J., Mpelasoka, F., Mainuddin, M., Ticehurst, C., Dyce, P., Hodgson, G., Ali, R., and Kirby, M.: Mekong river basin water resources assessment: Impacts of climate change, Water for a Healthy Country National Research Flagship, CSIRO (Commonwealth Scientific and Industrial Research Organization), Canberra, Australia, p. 153, 2008.

FAO – Food and Agriculture Organization of the United Nations: Digital agricultural atlas of Myanmar, http://dwms.fao.org/atlases/myanmar/index_en.htm (last access: 5 January 2013), 2008.

Fowler, H. J. and Archer, D. R.: Conflicting Signals of Climatic Change in the Upper Indus Basin, J. Climate, 9, 4276–4293, 2005.

Fritsch, J. M., Hilliker, J., Ross, J., and Vislocky, R. L.: Model consensus, Weather Forecast., 15, 571–582, 2000.

Giorgi, F.: Regional climate modeling: Status and perspectives, J. Phys. IV, 139, 101–118, 2006.

Giorgi, F. and Mearns, L. O.: Calculation of average, uncertainty range, and reliability of regional climate changes from AOGCM simulations via the "Reliability Ensemble Average" (REA) method, J. Climate, 15, 1141–1158, 2002

Gordon, H. B., Rotstayn, L. D., McGregor, J. L., Dix, M. R., Kowalczyk, E. A., O'Farrell, S. P., Waterman, L. J., Hirst, A. C., Wilson, S. G., Collier, M. A., Watterson, I. G. and, Elliott, T. I.: The CSIRO Mk3 climate system model, Tech. Pap. 60, Commonw. Sci. and Indust. Res.

ESDD
4, 109–177, 2013

Organ. Atmos. Res., http://www.cmar.csiro.au/e-print/open/gordon_2002a.pdf, last access: 5 January 2013, Aspendale, Victoria, Australia, 130 pp., 2002.
Gosain, A. K., Rao, S., and Basuray, D.: Climate change impact assessment on hydrology of Indian river basins, Current Sci., 90, 346–353, 2006.
Gurung, D. R., Amarnath, G., Khun, S. A., Shrestha, B., and Kulkarni, A. V.: Snow-cover mapping and monitoring in the Hindu Kush-Himalayas, ICIMOD, Kathmandu, 2011.
Hagemann, S., Arpe, K., and Roeckner, E.: Evaluation of the Hydrological Cycle in the ECHAM5 Model, J. Climate, 19, 3810–3827, 2006.
Harrison, M. S. J., Palmer, T. N., Richardson, D. S., and Buizza, R.: Analysis and model dependencies in medium-range ensembles: Two transplant case-studies, Q. J. Roy. Meteorol. Soc., 125, 2487–2515, 1999.
Hodges, I. K., Hoskins, B. J., Boyle, J., and Thorncroft, C.: A Comparison of Recent Reanalysis Datasets Using Objective Feature Tracking: Storm Tracks and Tropical Easterly Waves, Mon. Weather Rev. 131, 2012–2037, 2003.
Houghton, J. T., Ding, Y., Griggs, D. J., Noguer, M., van der Linden, P. J., and Xiaosu, D. (Eds.): Climate Change 2001: The Scientific Basis: Contributions of Working Group I to the Third Assessment Report of the Intergovernmental Panel on Climate Change, Cambridge University Press, 881 pp., 2001.
Immerzeel, W. W.: Historical trends and future predictions of climate variability in the Brahmaputra basin, Int. J. Climatol., 28, 243–254, doi:10.1002/joc.1528, 2008.
Immerzeel, W. W., Droogers, P., de Jong, S. M., and Bierkens, M. F. P.: Large-scale monitoring of snow cover and runoff simulation in Himalayan river basins using remote sensing, Remote Sens. Environ., 113, 40–49, 2009.
Immerzeel, W. W., van Beek, L. P. H., and Bierkens, M. F. P.: Climate change will affect the Asia Water Towers, Science, 328, 1382, doi:10.1126/science.1183188, 2010.
IPCC AR4: Climate change 2007: Impacts, adaptation and vulnerability, Cambridge University Press, Cambridge, 2007.
Islam, S., Rehman, N., Sheikh, M. M., and Khan, A. M.: Climate Change Projections for Pakistan, Nepal and Bangladesh for SRES A2 and A1B Scenarios using outputs of 17 GCMs used in IPCC-AR4, GCISC-RR-03, Global Change Impact Studies Centre (GCISC), Islamabad, Pakistan, 2009.

ESDD
4, 109–177, 2013

Hydrological cycle over south and southeast Asian river basins

S. Hasson et al.

Jian, J., Webster, P. J., and Hoyos, C. D.: Large-scale controls on Ganges and Brahmaputra River discharge on interaseasonal and seasonal time-scales, Q. J. Roy. Meteorol. Soc., 135, 353–370, 2009.
Johns, T. C., Gregory, J. M., Ingram, W. J., Johnson, C. E., Jones, A., Lowe, J. A., Mitchell, J. F. B., Roberts, D. L., Sexton, D. M. H., Stevenson, D. S., Tett, S. F. B., and Woodage, M. J.: Anthropogenic climate change for 1860 to 2100 simulated with the HadCM3 model under updated emissions scenarios, Clim. Dynam., 20, 583–612, 2003.
Johns, T. C., Durman, C. F., Banks, H. T., Roberts, M. J., McLaren, A. J., Ridley, J. K., Senior, C. A., Williams, K. D., Jones, A., Rickard, G. J., Cusack, S., Ingram, W. J., Crucifix, M., Sexton, D. M. H., Joshi, M. M., Dong, B.-W., Spencer, H., Hill, R. S. R., Gregory, J. M., Keen, A. B., Pardaens, A. K., Lowe, J. A., Bodas-Salcedo, A., Stark, S., and Searl, Y.: The new Hadley Centre climate model Had-GEM1: Evaluation of coupled simulations, J. Climate, 19, 1327–1353, 2006.
Johnston, R., Lacombe, G., Hoanh, C. T., Noble, A., Pavelic, P., Smakhtin, V., Suhardiman, D., Kam, S. P., and Choo, P. S.: Climate change, water and agriculture in the Greater Mekong Subregion, IWMI Research Report 136, International Water Management Institute, Colombo, Sri Lanka, p. 60, doi:10.5337/2010.212, 2010
Jungclaus, J., Botzet, M., Haak, H., Keenlyside, N., Luo, J. J., Latif, M., Marotzke, J., Mikolajewicz, J., and Roeckner, E.: Ocean circulation and tropical variability in the AOGCM ECHAM5/MPI-OM, J. Climate, 19, 3952–3972, 2006.
Kang, I.-S., Jin, K., Wang, B., Lau, K.-M., Shukla, J., Krishnamurthy, V., Schubert, S. D., Wailser, D. E., Stern, W. F., Kitoh, A., Meehl, G. A., Kanamitsu, M., Galin, V. Y., Satyan, V., Park, C.-K., and Liu, Y.: Intercomparison of the climatological variations of Asian summer monsoon precipitation simulated by 10 GCMs, Clim. Dynam., 19, 383–395, 2002.
Karim, A. and Veizer, J.: Water balance of the Indus River Basin and moisture source in the Karakoram and western Himalayas: Implications from hydrogen and oxygen isotopes in river water, J. Geophys. Res., 107, 4362, doi:10.1029/2000JD000253, 2002.
Knox, J. C.: Large increases in flood magnitude in response to modest changes in climate, Nature, 361, 430–432, 1993.
Krasovskania, I. and Gottschalk, L.: Stability of river flow regimes, Nord. Hydrol., 23, 137–154, 1992.
Kripalani, R. H., Kulkarni, A., and Singh, S. V.: Association of the Indian Summer Monsoon with the Northern Hemishpere Mid-Latitude Circulation, Int. J. Climatol., 17, 1055–1067, 1997.

ESDD
4, 109–177, 2013

Hydrological cycle over south and southeast Asian river basins

S. Hasson et al.

K-1 Model Developers: K-1 coupled model (MIROC) description in K-1 Technical Report, vol. 1, edited by: Hasumi, H. and Emori, S., Center for Climate System Research, Univ. of Tokyo, 34 pp., 2004.

Liepert, B. G. and Previdi, M.: Do models and observations disagree on the rainfall response to global warming?, J. Climate, 22, 3156–3166, 2009.

Liepert, B. G. and Previdi, M.: Inter-model variability and biases of the global water cycle in CMIP3 coupled climate models, Environ. Res. Lett., 7, 014006, doi:10.1088/1748-9326/7/1/014006, 2012.

Lin, J.-L., Weickman, K. M., Kiladis, G. N., Mapes, B. E., Schubert, S. D., Suarez, M. J., Bacmeister, J. T., and Lee, M.-I.: Subseasonal Variability Associated with Asian Summer Monsoon Simulated by 14 IPCC AR4 Coupled GCMs, J. Climate, 21, 4541–4567, doi:10.1175/2008JCLI1816.1, 2008.

Lucarini, V. and Ragone, F.: Energetics of climate models: Net energy balance and meridional enthalpy transport, Rev. Geophys., 49, RG1001, doi:10.1029/2009RG000323, 2011.

Lucarini, V. and Russell, G. L.: Comparison of mean climate trends in the northern hemisphere between National Centers for Environmental Prediction and two atmosphere-ocean model forced runs, J. Geophys. Res., 107, 4269, doi:10.1029/2001JD001247, 2002.

Lucarini, V., Danihlik, R., Kriegerova, I., and Speranza, A.: Does the Danube exist? Versions of reality given by various regional climate models and climatological datasets, J. Geophys. Res., 112, D13103, doi:10.1029/2006JD008360, 2007a.

Lucarini, V., Calmanti, S., Dell'Aquila, A., Ruti, P. M., and Speranza, A.: Intercomparison of the northern hemisphere winter mid-latitude atmospheric variability of the IPCC models, Clim. Dynam., 28, 829–848, doi:10.1007/s00382-006-0213-x, 2007b.

Lucarini, V., Danihlik, R., Kriegerova, I., and Speranza, A.: Hydrological cycle in the Danube basin in present-day and XXII century simulations by IPCCAR4 global climate models, J. Geophys. Res., 113, D09107, doi:10.1029/2007JD009167, 2008.

Marti, O., Braconnot, P., Bellier, J., Benshila, R., Bony, S., Brockmann, P., Cadule, P., Caubel, A., Denvil, S., Dufresne, J. L., Fairhead, L., Filiberti, M.-A., Foujols, M.-A., Fichefet, T., Friedlingstein, P., Goosse, H., Grandpeix, J. Y., Hourdin, F., Krinner, G., Lévy, C., Madec, G., Musat, I., de Noblet, N., Polcher, J., and Talandier, C.: The new IPSL climate system model: IPSL-CM4, Tech. Rep., Institut Pierre Simon Laplace des Sciences de l'Environnement Global (IPSL), Paris, France, 2005.

May, W.: Simulated changes of the Indian summer monsoon under enhanced greenhouse gas conditions in a global time-slice experiment, Geophy. Res. Lett., 29, 1118, doi:10.1029/2001GL013808, 2002.
Meehl, G. A., Washington, W. M., Ammann, C., Arblaster, J. M., and Wigley, T. M. L.: Combinations of natural and anthropogenic forcings and 20th century climate, J. Climate, 17, 3721–3727, 2004.
Miller, J. R. and Russell, G. L.: The impact of global warming on river runoff, J. Geophys. Res., 97, 2757–2764, 1992.
Min, S. K., Legutke, S., Hense, A., and Kwon, W. T.: Internal variability in a 1000-year control simulation with the coupled climate model ECHO-G, Part I. Near-surface temperature, precipitation and mean sea level pressure, Tellus A, 57, 605–621, 2005.
Mirza, M. Q., Warrick, R. A., Ericksen, N. J., and Kenny, G. J.: Trends and persistence in precipitation in the Ganges, Brahmaputra and Meghna river basins, Hydrolog. Sci. J., 43, 845–858, 1998.
MRC: Overview of the Hydrology of the Mekong Basin, Lao PDR, Mekong River Commission, Vientiane, November 2005.
Nijssen, B., O'Donnell, G. M., Hamlet, A. F., and Lettenmaier, D. P.: Hydrological Sensitivity of Global Rivers to Climate Change, Climatic Change, 50, 143–175, 2001.
Nohara, D., Kitoh, A., Hosaka, A. M., and Oki, T.: Impact of Climate Change on River Discharge Projected by Multimodel Ensemble, J. Hydrometeorol., 7, 1076–1089, doi:10.1175/JHM531.1, 2006.
Okabe, A., Boots, B., Sugihara, K., and Chiu S. N.: Spatial Tessellations – Concepts and Applications of Voronoi Diagrams, John Wiley and Sons, New York, USA, 2000.
Parry, M. L., Carter, T. L., and Konijn, M. (Eds.): The impact of climatic variations on agriculture, 1, cool and temperature regions, Kluwer, Norwell, Mass., 1988.
Peixoto, J. P. and Oort, A. H.: Physics of Climate, American Institute of Physics, New York, 1992.
Previdi, M. and Liepert, B. G.: Annular modes and Hadley cell expansion under global warming, Geophys. Res. Lett., 34, L22701, doi:10.1029/2007GL031243, 2007.
Rees, H. G. and Collins, D. N.: Regional differences in response of flow in glacier-fed Himalayan Rivers to climatic warming, Hydrol. Process., 20, 2157–2169, 2006.

ESDD
4, 109–177, 2013

Salas-Meélia, D., Chauvin, F., Deéqueé, M., Douville, H., Gueremy, J. F., Marquet, P., Planton, S., Royer, J. F., and Tyteca, S.: Description and validation of the CNRM-CM3 global coupled model, CNRM working note 103, Toulouse, France, 2005.
Scherler, D., Bookhagen, B., and Strecker, M. R.: Spatially variable response of Himalayan glaciers to climate change affected by debris cover, Nat. Geosci., 4, 156–159, 2011.
Singh, P. and Bengtsson, L.: Hydrological sensitivity of a large Himalayan basin to climate change, Hydrol. Process., 18, 2363–2385, doi:10.1002/hyp.1468, 2004.
Singh, P. and Kumar, N.: Impact assessment of climate change on the hydrological response of a snow and glacier melt runoff dominated Himalayan river, J. Hydrol., 193, 316–350, 1997.
Singh, P., Arora, M., and Goel, N. K.: Effect of climate change on runoff of a glacierized Himalayan basin, Hydrol. Process., 20, 1979–1992, doi:10.1002/hyp.5991, 2006.
Stowasser, M., Annamalai, H. and Hafner, J.: Response of the South Asian Summer Monsoon to Global Warming: Mean and Synoptic Systems, J. Climate, 22, 1014–1036, 2007.
Turner, A. G. and Annamalai, H.: Climate change and the sout-Asian summer monsoon, Nat. Climate Change, 2, 587–595, 2012.
Volodin, E. M. and Diansky, N. A.: El-Nino reproduction in coupled general circulation model of atmosphere and ocean, Russ. Meteorol. Hydrol., 12, 5–14, 2004.
Webster, P. J., Magaña, V. O., Palmer, T. N., Shukla, J., Tomas, R. A., Yanai, M., and Yasunari, T.: Monsoons: Processes, predictability, and the prospects for prediction, J. Geophys. Res., 103, 14451–14510, 1998.
Yukimoto, S. and Noda, A.: Improvements of the Meteorological Research Institute Global Ocean-atmosphere Coupled GCM (MRICGCM2) and its climate sensitivity, Tech. Rep. 10, NIES, Japan, 2002.
Zickfed, K., Knopf, B., Petoukhov, V., Schellnhuber, H. J.: Is the Indian summer monsoon stable against global change? Geophys. Res. Lett., 32, L15707, doi:10.1029/2005GL022771, 2005.

ESDD
4, 109–177, 2013

Hydrological cycle over south and southeast Asian river basins

S. Hasson et al.

Table 1. Characteristics of four studied river basins.

Basin characteristics	Indus	Ganges	Brahmaputra	Mekong
Basin area (km^2)	1 230 000	1 000 000	530 000	840 000
River length (km)	3200	2500	2900	4800
Near-to-sea gauge used in study	Kotri	Hardinge Bridge	Bahadurabad	Pakse
Annual mean discharge ($m^3 s^{-1}$)	1250	11 000	20 000	17 000
Peak discharge month	August	August	July	August
High flow season	April–September	July–October	April–November	June–November
No of glaciers/area (km^2)	18 495/21 000	7963/9000	11 497/14 000	482/230
Snow coverage (Annual avg. %)	13.5	5	20	3
Snow and glacier melt index	150	10	27	Negligible
Population dependent (millions)	260	520	66	79
Major consumption	Agriculture	Agriculture	Agriculture	Agriculture
Seasonal/annual Variability	High	High	High	High

ESDD
4, 109–177, 2013

Table 2. List of GCMs used in the study. These constitute the subset of all GCMs included in the PCMDI/CMIP3 project providing all the climate variables of our interest.

Name and reference	Institution	Grid resolution (Lat × Lon)
CNRMCM Salas-Meélia et al. (2005)	Météo-France/Centre National de Recherches Météorologiques, France	T63
MRI-CGCM2.3.2 Yukimoto and Noda (2002)	Meteorological Research Institute, Japan Meteorological Agency, Japan	T42
CSIRO3.0 Gordon et al. (2002)	CSIRO Atmospheric Research, Australia	T63
ECHAM5 Jungclaus et al. (2006)	Max Planck Institute for Meteorology, Germany	T63
ECHOG Min et al. (2005)	MIUB, METRI, and M&D, Germany/Korea	T30
GFDL20 Delworth et al. (2005)	US Dept. of Commerce/NOAA Geophysical Fluid Dynamics Laboratory, USA	$2.5^\circ \times 2.0^\circ$
GISSAOM Lucarini and Russell (2002)	NASA/Goddard Institute for Space Studies, USA	$4^\circ \times 3^\circ$
INMCM30 Volodin and Diansky (2004)	Institute for Numerical Mathematics, Russia	$5^\circ \times 4^\circ$
IPSL-CM4 Marti et al. (2005)	Institute Pierre Simon Laplace, France	$2.4^\circ \times 3.75^\circ$
MIROC (hires) K-1 Model Developers (2004)	CCSR/NIES/FRCGC, Japan	T106
PCM1MODEL Meehl et al. (2004)	National Centre for Atmospheric Research, USA	T42
UKMOHADCM3 Johns et al. (2003)	Hadley Centre for Climate Prediction and Research/Met Office, UK	$2.75^\circ \times 3.75^\circ$
UKMOHADGEM3 Johns et al. (2006)	Hadley Centre for Climate Prediction and Research/Met Office, UK	$1.25^\circ \times 1.875^\circ$

ESDD
4, 109–177, 2013

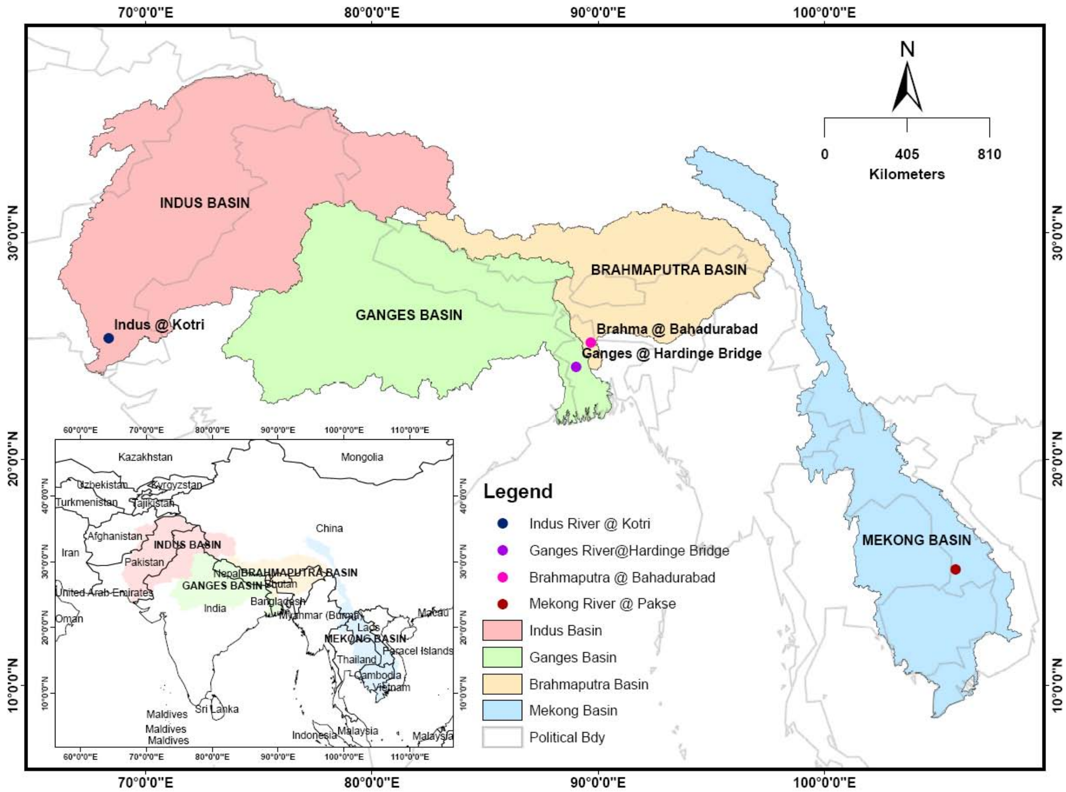

Fig. 1. Four study river basins; Indus, Ganges, Brahmaputra and Mekong (west to east).

ESDD
4, 109–177, 2013

Hydrological cycle over south and southeast Asian river basins

S. Hasson et al.

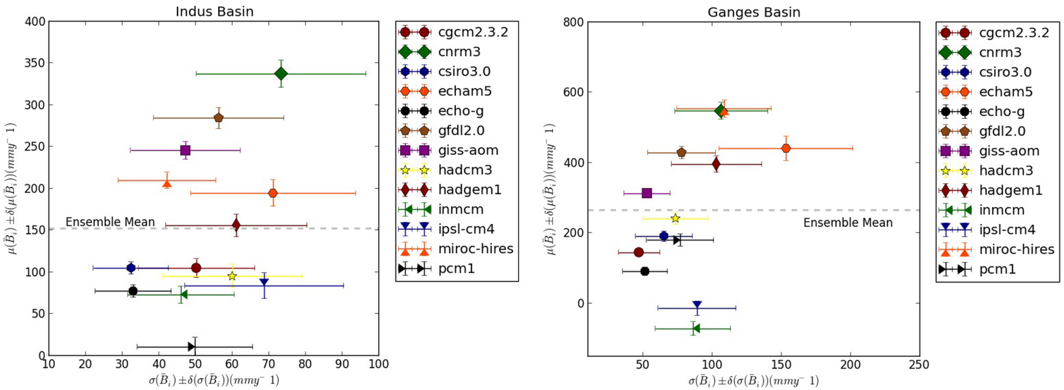

Fig. 2. Inter-annual variability versus mean annual basin-integrated water balance (markers) for historical climate (1961–2000) and their 95 % confidence intervals (lines) **(a)** Indus Basin – observed long-term averaged discharge at sea is about 30 mm yr^{-1}. Note that 100 mm yr^{-1} corresponds to about 3890 m^3 s^{-1} of the equivalent mean Indus discharge **(b)** Ganges Basin – observed long-term averaged discharge at sea is about 345 mm yr^{-1}. Note that 100 mm yr^{-1}corresponds to about 3190 m^3 s^{-1} of the equivalent mean Ganges discharge.

ESDD
4, 109–177, 2013

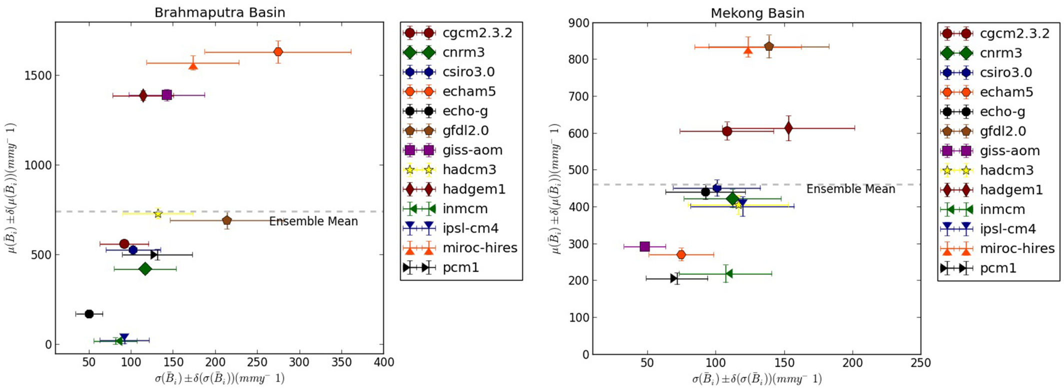

Fig. 3. Inter-annual variability versus mean annual basin-integrated water balance (markers) (1961–2000) and their 95 % confidence intervals (lines) for **(a)** Brahmaputra Basin – observed long-term averaged discharge at sea is about 1200 mm yr^{-1}. Note that 100 mm yr^{-1} corresponds to about 1680 m^3 s^{-1} of the equivalent mean Brahmaputra discharge **(b)** Mekong Basin – observed long-term averaged discharge at sea is about 650 mm yr^{-1}. Note that 100 mm yr^{-1} corresponds to about 2670 m^3 s^{-1} of the equivalent mean Mekong discharge.

ESDD

4, 109–177, 2013

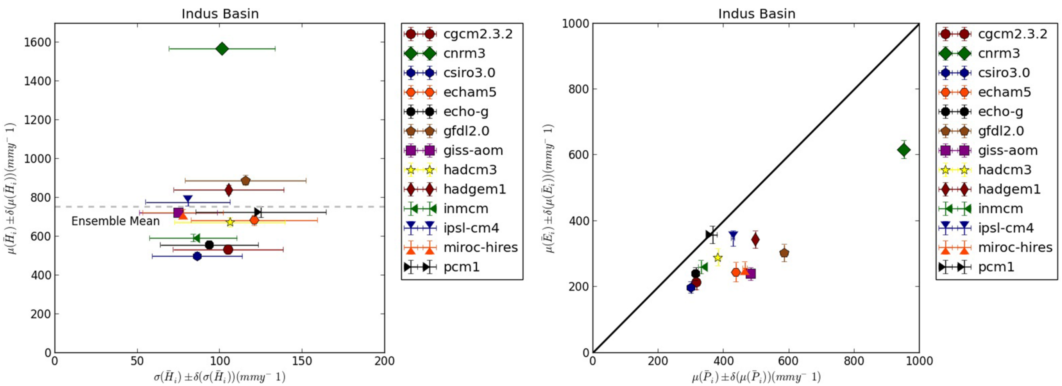

Fig. 4. Inter-annual variability versus mean annual basin-integrated strength of hydrological cycle **(a)** and mean annual basin-integrated evaporation versus mean annual basin-integrated precipitation **(b)** for Indus Basin (1961–2000) (markers) and their 95 % confidence intervals (lines). Note that 100 mm yr^{-1} corresponds to about 3890 m^3 s^{-1} of the equivalent mean Indus discharge.

ESDD
4, 109–177, 2013

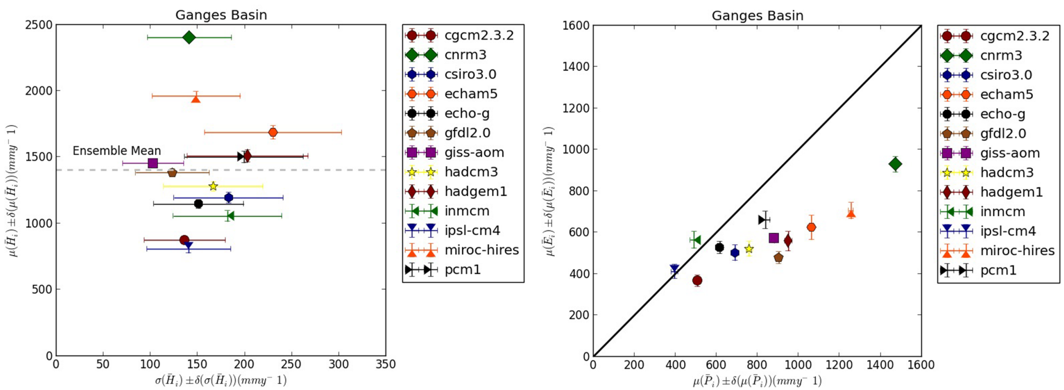

Fig. 5. Inter-annual variability versus mean annual basin-integrated strength of hydrological cycle **(a)** and mean annual basin-integrated evaporation versus mean annual basin-integrated precipitation **(b)** for Ganges Basin (1961–2000) (markers) and their 95 % confidence intervals (lines). Note that 100 mm yr^{-1} corresponds to about 3190 m^3 s^{-1} of the equivalent mean Ganges discharge.

ESDD

4, 109–177, 2013

Hydrological cycle over south and southeast Asian river basins

S. Hasson et al.

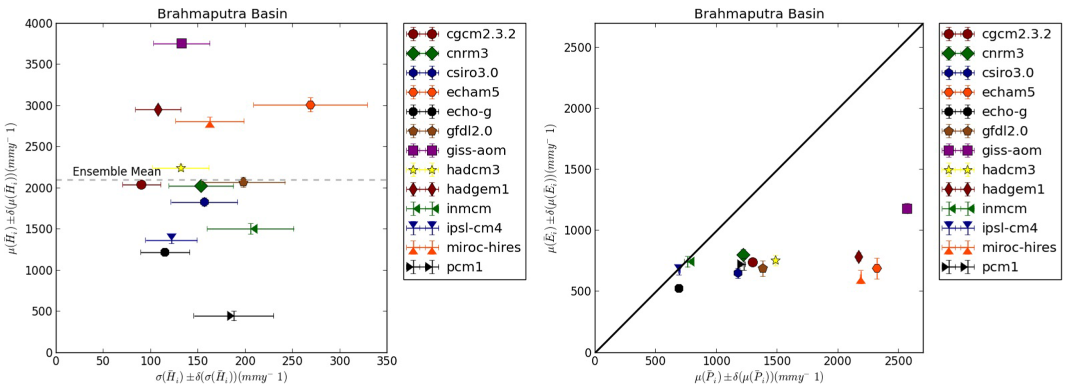

Fig. 6. Inter-annual variability versus mean annual basin-integrated strength of hydrological cycle **(a)** and mean annual basin-integrated evaporation versus mean annual basin-integrated precipitation **(b)** for Brahmaputra Basin (1961–2000) (markers) and their 95 % confidence intervals (lines). Note that 100 mm yr^{-1} corresponds to about 1680 m^3 s^{-1} of the equivalent mean Brahmaputra discharge.

ESDD
4, 109–177, 2013

Hydrological cycle over south and southeast Asian river basins

S. Hasson et al.

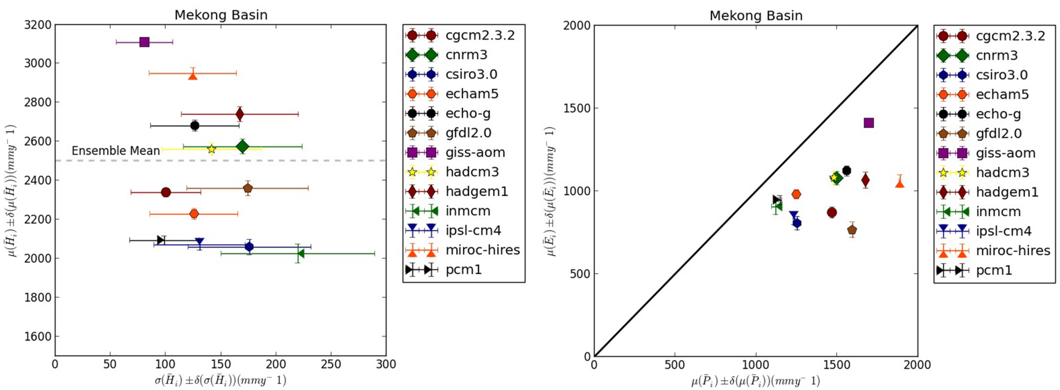

Fig. 7. Inter-annual variability versus mean annual basin-integrated strength of hydrological cycle **(a)** and mean annual basin-integrated evaporation versus mean annual basin-integrated precipitation **(b)** for Mekong Basin (1961–2000) (markers) and their 95 % confidence intervals (lines). Note that 100 mm yr^{-1} corresponds to about 2670 m^3 s^{-1} of the equivalent mean Mekong discharge.

ESDD

4, 109–177, 2013

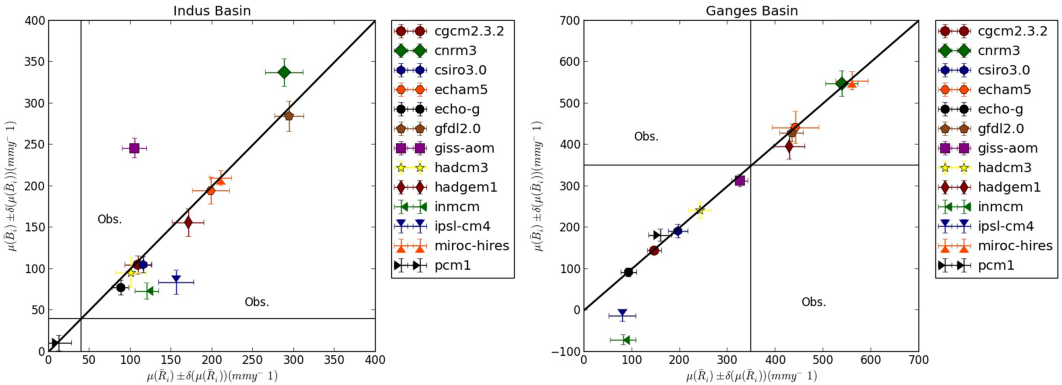

Fig. 8. Mean annual basin-integrated total runoff (surface + sub-surface) versus estimated mean annual basin-integrated water balance (markers) and their 95 % confidence intervals (lines) for (1961–2000) **(a)** Indus Basin – observed long-term averaged discharge at sea is about 30 mm yr^{-1}. Note that 100 mm yr^{-1} corresponds to about 3890 m^3 s^{-1} of the equivalent mean Indus discharge, **(b)** Ganges Basin – observed long-term averaged discharge at sea is about 345 mm yr^{-1}. Note that 100 mm yr^{-1} corresponds to about 3190 m^3 s^{-1} of the equivalent mean Ganges discharge.

ESDD
4, 109–177, 2013

Hydrological cycle over south and southeast Asian river basins

S. Hasson et al.

Title Page
Abstract | Introduction
Conclusions | References
Tables | Figures
◂◂ | ▸▸
◂ | ▸
Back | Close
Full Screen / Esc
Printer-friendly Version
Interactive Discussion

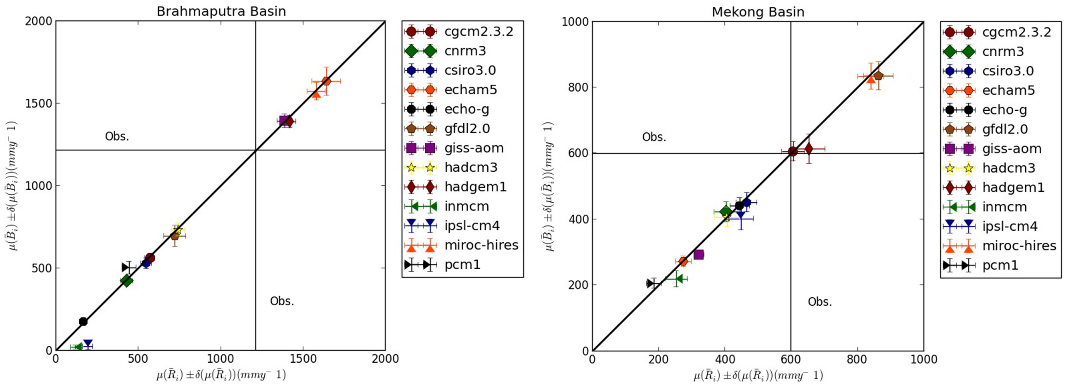

Fig. 9. Mean annual basin-integrated total runoff (surface + sub-surface) versus estimated mean annual basin-integrated water balance (markers) and their 95 % confidence intervals (lines) for (1961–2000) **(a)** Brahmaputra Basin – observed long-term averaged discharge at sea is about 1200 mm yr^{-1}. Note that 100 mm yr^{-1} corresponds to about 1680 m^3 s^{-1} of the equivalent mean Indus discharge **(b)** Mekong Basin – observed long-term averaged discharge at sea is about 650 mm yr^{-1}. Note that 100 mm yr^{-1} corresponds to about 2670 m^3 s^{-1} of the equivalent mean Indus discharge.

ESDD
4, 109–177, 2013

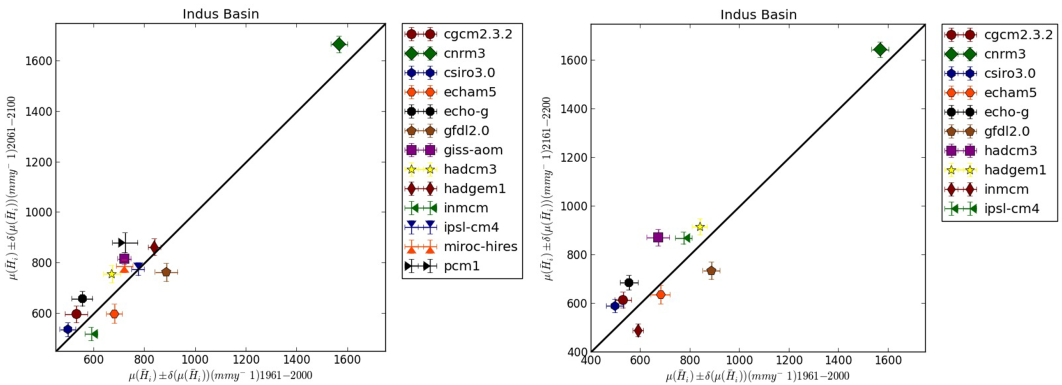

Fig. 10. Indus Basin mean annual basin-integrated estimated strength of hydrological cycle relative to XX century (1961–2000) (markers) and their 95 % confidence intervals (lines) for XXI century (2061–2100) (left panel) and for XXII century (2161–2200) (right panel).

ESDD

4, 109–177, 2013

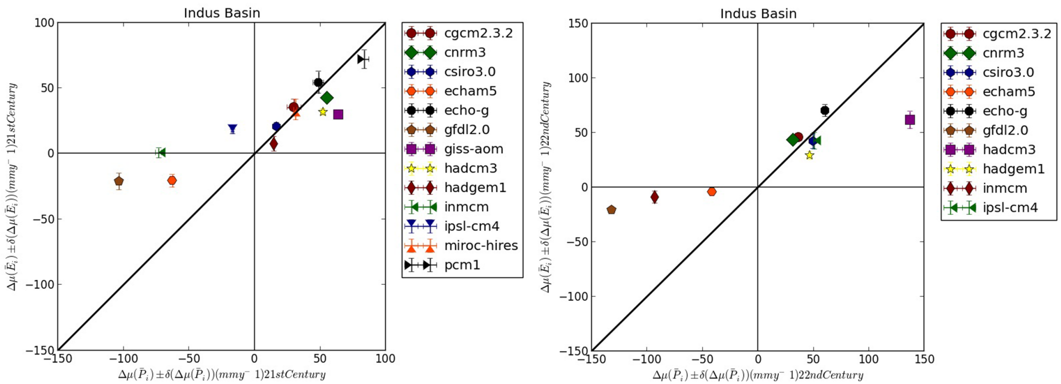

Fig. 11. Change in mean annual basin-integrated estimated precipitation versus change in its mean annual basin-integrated estimated evaporation (markers) and their 95 % confidence intervals (lines) by XXI century (2061–2100) (left panel) and for XXII century (2161–2200) (right panel) relative to XX century (1961–2000) for Indus Basin.

ESDD
4, 109–177, 2013

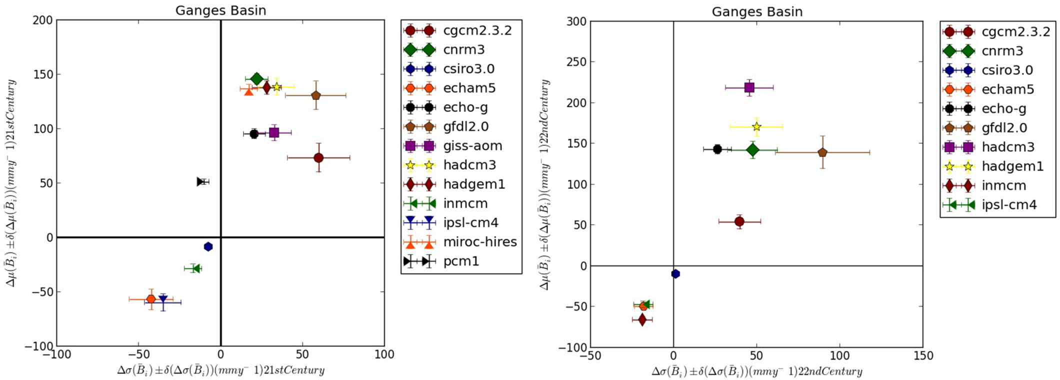

Fig. 12. Change in mean annual basin-integrated estimated water balance versus change in its inter-annual variability (markers) and their 95 % confidence intervals (lines) by XXI century (2061–2100) (left panel) and for XXII century (2161–2200) (right panel) relative to XX century (1961–2000) for the Ganges Basin.

ESDD
4, 109–177, 2013

Hydrological cycle over south and southeast Asian river basins

S. Hasson et al.

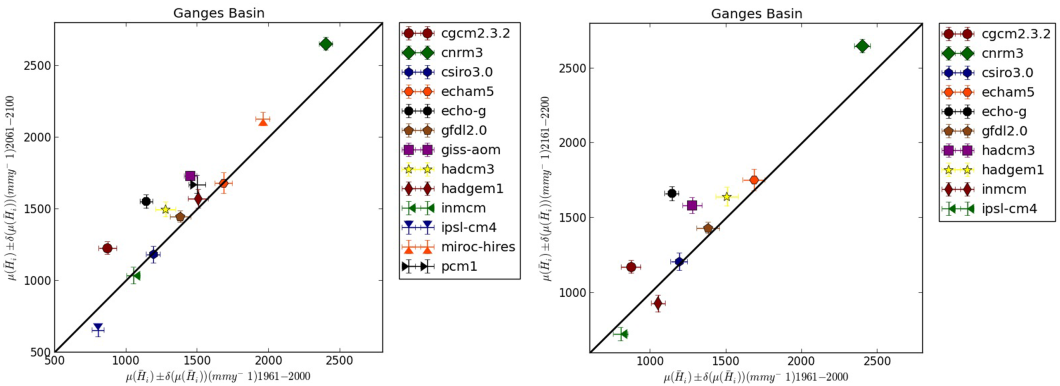

Fig. 13. Ganges Basin mean annual basin-integrated estimated strength of hydrological cycle relative to XX century (1961–2000) (markers) and their 95 % confidence intervals (lines) for XXI century (2061–2100) (left panel) and for XXII century (2161–2200) (right panel).

ESDD

4, 109–177, 2013

Hydrological cycle over south and southeast Asian river basins

S. Hasson et al.

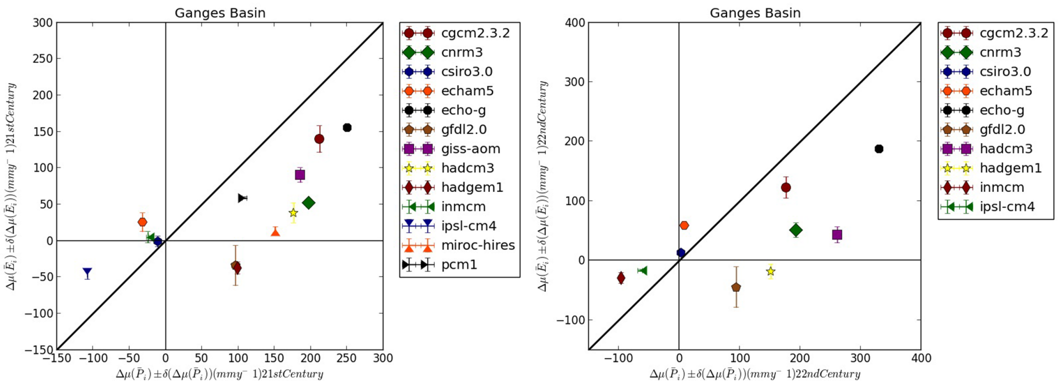

Fig. 14. Change in mean annual basin-integrated estimated precipitation versus change in its mean annual basin-integrated estimated evaporation (markers) and their 95 % confidence intervals (lines) by XXI century (2061–2100) (left panel) and for XXII century (2161–2200) (right panel) relative to XX century (1961–2000) for the Ganges Basin.

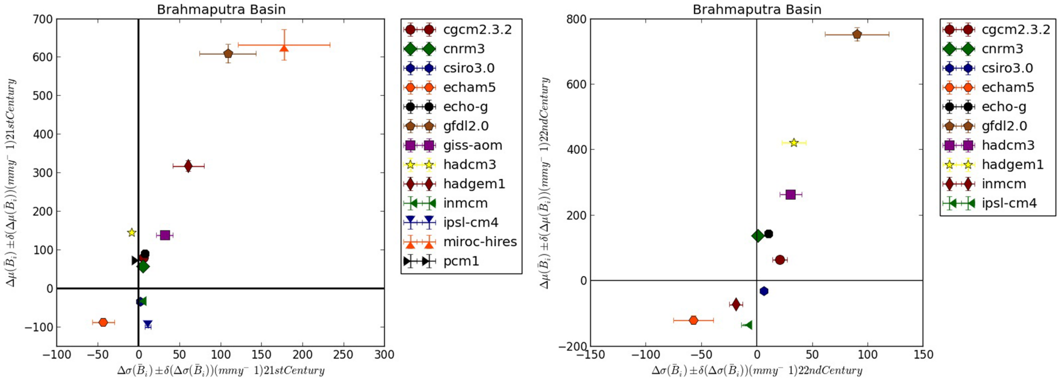

Fig. 15. Change in mean annual basin-integrated estimated water balance versus change in its inter-annual variability (markers) and their 95 % confidence intervals (lines) by XXI century (2061–2100) (left panel) and for XXII century (2161–2200) (right panel) relative to XX century (1961–2000) for the Brahmaputra Basin.

ESDD
4, 109–177, 2013

Title Page
Abstract | Introduction
Conclusions | References
Tables | Figures
◀| |▶
◀ ▶
Back | Close
Full Screen / Esc
Printer-friendly Version
Interactive Discussion

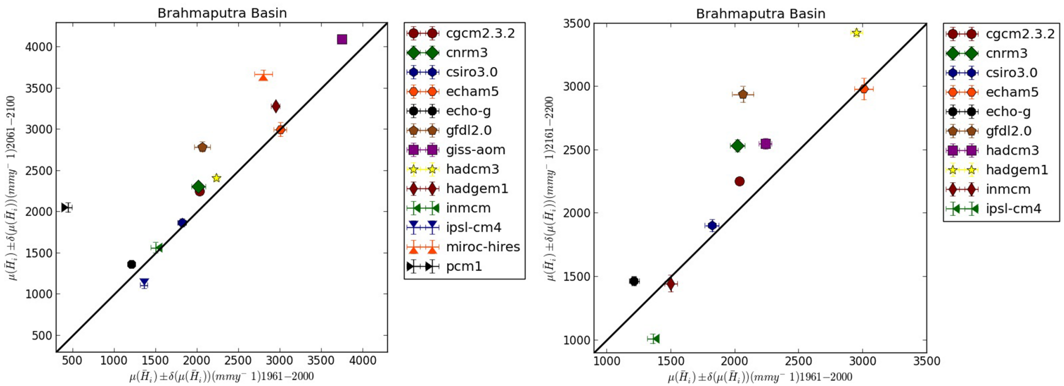

Fig. 16. Brahmaputra Basin mean annual basin-integrated estimated strength of hydrological cycle relative to XX century (1961–2000) (markers) and their 95 % confidence intervals (lines) for XXI century (2061–2100) (left panel) and for XXII century (2161–2200) (right panel).

Discussion Paper | Discussion Paper | Discussion Paper | Discussion Paper |
ESDD
4, 109–177, 2013
Hydrological cycle over south and southeast Asian river basins
S. Hasson et al.

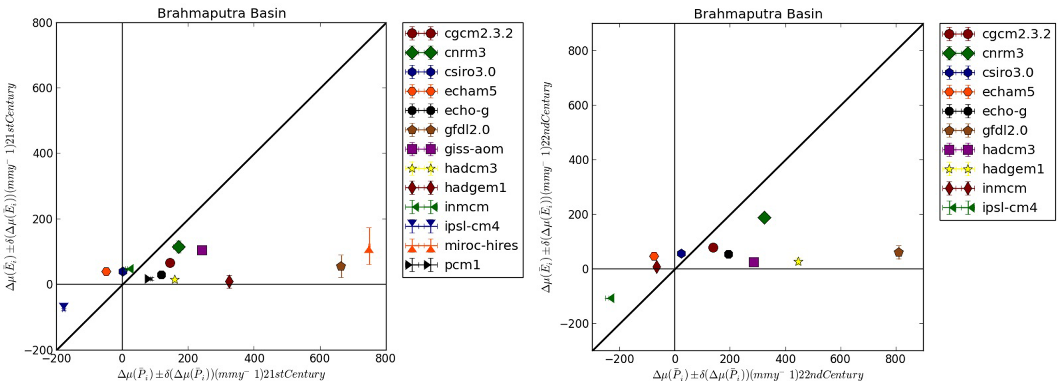

Fig. 17. Change in mean annual basin-integrated estimated precipitation versus change in its mean annual basin-integrated estimated evaporation (markers) and their 95 % confidence intervals (lines) by XXI century (2061–2100) (left panel) and for XXII century (2161–2200) (right panel) relative to XX century (1961–2000) for Brahmaputra Basin.

ESDD
4, 109–177, 2013

Hydrological cycle over south and southeast Asian river basins

S. Hasson et al.

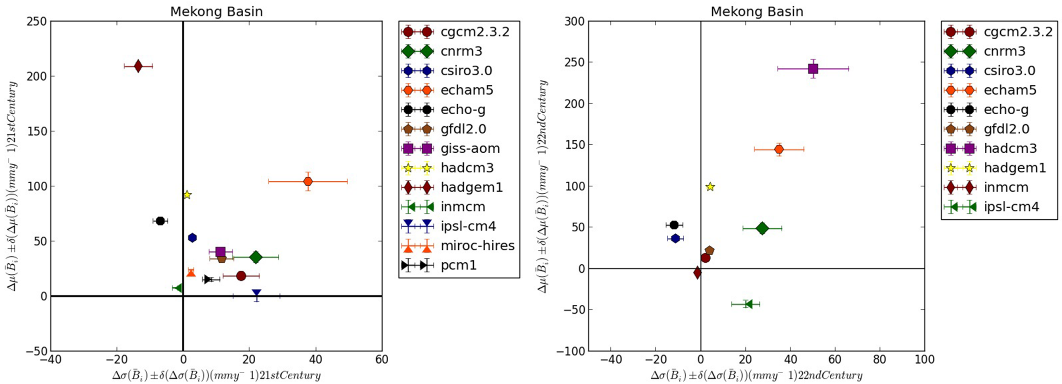

Fig. 18. Change in mean annual basin-integrated estimated water balance relative to XX century (1961–2000) versus change in its inter-annual variability (markers) and their 95 % confidence intervals (lines) for XXI century (2061–2100) (left panel) and for XXII century (2161–2200) (right panel) Mekong Basin.

ESDD
4, 109–177, 2013

Hydrological cycle over south and southeast Asian river basins

S. Hasson et al.

Title Page
Abstract
Introduction
Conclusions
References
Tables
Figures
◀
▶
Back
Close
Full Screen / Esc
Printer-friendly Version
Interactive Discussion

ESDD
4, 109–177, 2013

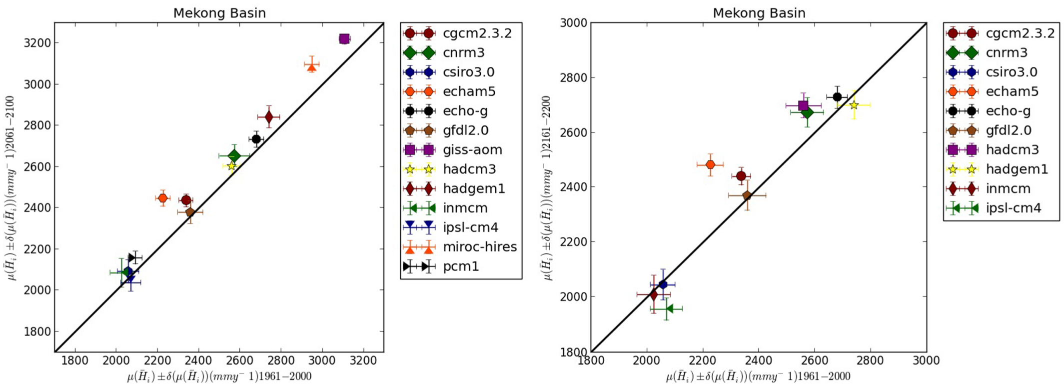

Fig. 19. Mean annual basin-integrated estimated strength of hydrological cycle relative to XX century (1961–2000) (markers) and their 95 % confidence intervals (lines) for XXI century (2061–2100) (left panel) and for XXII century (2161–2200) (right panel) for Mekong Basin.

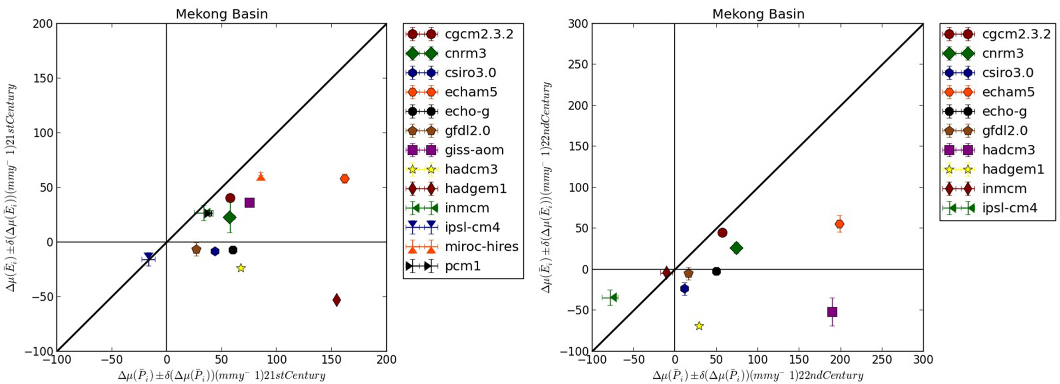

Fig. 20. Mean annual basin-integrated evaporation versus mean annual basin-integrated precipitation (markers) and their 95 % confidence intervals (lines) for Mekong Basin for XXI century (2061–2100) (left panel) and for XXII century (2161–2200) (right panel).

ESDD
4, 109–177, 2013